Limitation by Fe, Zn, Co, and B$_{12}$ Results in Similar Physiological Responses in Two Antarctic Phytoplankton Species

Florian Koch[1,2]* and Scarlett Trimborn[1,3]

[1] Alfred Wegener Institute Helmholtz Zentrum für Polar und Meeresforschung, Bremerhaven, Germany, [2] Fachbereich 1, University of Applied Sciences, Bremerhaven, Germany, [3] Marine Botany, University of Bremen, Bremen, Germany

In many areas of the world's ocean such as the Southern Ocean (SO), primary production is low despite an abundance of macronutrients. In these high nutrient low chlorophyll (HNLC) regions the trace metal (TM) iron (Fe) limits phytoplankton biomass and subsequently the biological carbon pump. Besides Fe, the TMs zinc (Zn), cobalt (Co), and the vitamin cobalamin (B$_{12}$) have also been shown to limit biomass and/or influence plankton species composition. While the impacts of Fe limitation and, to a lesser degree of Zn and Co, on the cellular physiology of Antarctic phytoplankton have been investigated, studies focusing simultaneously on several TMs and vitamins are still lacking. This study measured the impacts of Fe, Zn, Co, and B$_{12}$ limitation on the Antarctic diatom *Chaetoceros simplex* and Fe and Zn limitation on the Antarctic cryptophyte *Geminigera cryophila*. Both species responded to all limitation scenarios by reducing their growth and particulate organic carbon (POC) production rates. For both algae limitation by Fe and Zn resulted in a reduction of light harvesting pigments, a significant reduction in the photosynthetic yield (F_v/F_m) and increase in the C:N ratio. Most interestingly, with a few exceptions, limitation by one TM also resulted in a significant decrease of the cellular quotas of other TMs measured. These observations suggest that one consequence of limitation by one TM may be a secondary and perhaps more fatal limitation by another.

Keywords: Southern Ocean, trace metals, phytoplankton, vitamins, B$_{12}$, iron, zinc, cobalt

INTRODUCTION

In large areas of the world's ocean, phytoplankton biomass is low despite of a plethora of macronutrients. In these high nutrient low chlorophyll (HNLC) regions, the plankton community experiences low concentrations of essential micronutrients such as iron (Fe, < nmol L^{-1}; Martin et al., 1990), zinc (Zn, nmol L^{-1}; Croot et al., 2011), cobalt (Co, pmol L^{-1}; Panzeca et al., 2009), and even vitamins, like cobalamin (B$_{12}$, pmol L^{-1}; Koch et al., 2011). These low concentrations can pose a challenge for the plankton community since many cellular metabolic enzymes require metals (Twining and Baines, 2013). Especially Fe is required for vital processes such as carbon and nitrogen fixation, nitrate and nitrite reduction, chlorophyll synthesis and is essential for the electron transport chain of respiration and photosynthesis (Raven et al., 1999; Behrenfeld and Milligan, 2013; Twining and Baines, 2013). Zn plays an important role in carbonic anhydrase,

an enzyme catalyzing the interconversion of CO_2 and bicarbonate for photosynthesis (Lionetto et al., 2016), and in alkaline phosphatase, an enzyme important in cleaving phosphate from larger organic molecules in times of phosphorus limitation (Dyhrman and Ruttenberg, 2006). Zinc-fingers are also important in DNA/RNA replication (Klug, 2010). Co is the central atom in the corrin-ring of the B_{12} molecule, making it an obligate trace metal (TM) for vitamin-producing bacteria (Banerjee and Ragsdale, 2003). Most phytoplankton (Croft et al., 2006; Tang et al., 2010) and bacteria (Sañudo-Wilhelmy et al., 2012) possess numerous B_{12}-requiring metabolic pathways such as the biosynthesis of the essential amino acid methionine. B_{12} is also essential in carbon transfer reactions and involved in DNA synthesis.

Even though Fe controls plankton biomass in the HNLC areas of the Southern Ocean (SO; i.e., Martin et al., 1990; de Baar et al., 2005), recent work highlights that it is not only the total concentration of Fe, but also the Fe source, which governs species composition (Browning et al., 2014; Conway et al., 2016; Trimborn et al., 2017), possibly due to varying bioavailability of the Fe itself (Hassler et al., 2012; Shaked and Lis, 2012). Alternatively, since Fe from dust, meltwater or upwelling is typically accompanied by the input of other TMs, the changing ratios of TMs may also impact the plankton community. Indeed several studies describe that other TMs alone or in conjunction with Fe can limit or co-limit productivity and/or shape plankton composition in HNLC regions (Moore et al., 2013). Zn additions have been reported to alter plankton communities in the and North Pacific (Coale, 1991; Crawford et al., 2003) while Co has been shown impact the plankton composition in the North Pacific (Martin et al., 1989), North Atlantic (Panzeca et al., 2008), and Southeast Atlantic (Browning et al., 2017). Similarly, B_{12} has been implicated in governing plankton biomass in the North Pacific (Koch et al., 2011; Heal et al., 2017), Southeast Atlantic (Browning et al., 2017), and SO (Panzeca et al., 2006; Bertrand et al., 2007, 2015).

As previously observed for *P. antarctica* (Koch et al., 2019; Trimborn et al., 2019a) and other phytoplankton species (Allen et al., 2008; Botebol et al., 2017; Blanco-Ameijeiras et al., 2018), Fe limitation significantly affects cellular physiology. Typically Fe-limited cells grow more slowly, are often smaller, alter their photophysiology and have reduced particulate organic carbon (POC) quotas. Other studies have described similar physiological responses of phytoplankton to limitation by Zn (Sunda and Huntsman, 1992; Sinoir et al., 2012, 2017), Co (Saito and Goepfert, 2008; Hawco and Saito, 2018), and B_{12} (Tang et al., 2010; Bertrand et al., 2012; Koch et al., 2013; Cohen et al., 2017). Some studies looked at the effects of limitation by one TM on the uptake/cellular quota of another (Sunda and Huntsman, 2004; Annett et al., 2008; Hawco and Saito, 2018). While these typically focused on the limitation of one or two TMS, they yielded important new concepts such as the biodilution of TMs (Sunda and Huntsman, 1998), the substitution of one TM for another (Sunda and Huntsman, 1995; Timmermans et al., 2001) and the classification of different limitation and co-limitation scenarios (Saito et al., 2008). A recent study (Koch et al., 2019) discovered that Fe limitation resulted in a significant decrease

of all other cellular TMs measured, not just Fe. It is unclear, however, if this phenomenon is specific to *P. antarctica* or if other SO phytoplankton groups respond similarly.

The diatom *Chaetoceros simplex*, and the cryptophyte *Geminigera cryophila*, two phytoplankton species isolated from the SO, were chosen to contrast the previous study conducted using *P. antarctica* (Koch et al., 2019). Both species were cultivated under different TM limitation (Fe, Zn, Co, and B_{12}) scenarios and the effects of each scenario on growth, elemental composition [C, N, Si, Fe, Zn, Co, manganese (Mn) and copper (Cu)] and photophysiology were assessed. This study shows that limitation by Fe, Zn, Co, and B_{12} resulted in similar physiological responses in both species. These include a decrease in growth and POC production rates, as well as a general reduction in the TM:C ratios of all TMs measured. For Fe- and Zn-limited cells, a reduction in light harvesting pigment quotas and changes in the photophysiology were observed.

MATERIALS AND METHODS

Culture Conditions

In order to minimize contamination, TM clean techniques were used for all aspects of this study. Cultures were grown in polycarbonate (PC) bottles, which had been sequentially soaked for 1 week in 1% Citranox® and for 2 weeks in 1 mol L^{-1} hydrochloric acid ("HPLC" grade, Merck Millipore Corporation, Darmstadt, Germany). Between each soaking step, the bottles were rinsed seven times with ultrapure water (Merck Millipore Corporation, Darmstadt, Germany). Finally, the TM cleaned equipment/bottles were air dried under a clean bench (US class 100, Opta, Bensheim, Germany) and packed in three polyethylene (PE) bags for storage. In order to precisely manipulate TM concentrations, the artificial seawater medium Aquil was used (Price et al., 1989). A concentrated (5x) inorganic salt solution was prepared, chelexed for 1 week (Chelex® 100, Sigma Aldrich, Merck, Darmstadt, Germany), diluted with ultrapure water to a salinity of 34, and fortified with chelexed macronutrients according to Price et al. (1989). To ensure that the TM being investigated had been effectively minimized in the artificial media, each individual batch of Aquil was checked by analyzing samples on an Inductively Coupled Plasma – Mass Spectrometer (ICP-MS, see full methods below; **Supplementary Table 1**). Prior to use, the medium was filter sterilized and a metal mix (made from Single-Element Standards, SCP Science, Quebec, Canada) was added for the control or, depending on the limitation scenario, modified by omitting either Fe, Zn, or Co, henceforth referred to as -Fe, -Zn, and -Co treatment, respectively. Similarly, in addition to the conventional vitamin mix (B_1, B_7, and B_{12}) used for the control, -Fe, -Zn, and -Co treatments, for the B_{12} limitation treatment (from now on referred to as -B_{12}), only B_1 and B_7 were added (Koch et al., 2013). As the aim of the study was to compare the effects of TM/vitamin limitation to ideal, nutrient replete growth conditions, concentrations of nutrients, TMs and vitamins in the media were, much higher than those found in the SO but typical for Aquil and other F/2 based medias (Wake et al., 2012). Additionally, to establish whether the omission of

one TM or vitamin changes the speciation of the others, the program MINEQL + (ver.4.5, Environmental Research Software, Hallowell, ME, United States) was used (Sinoir et al., 2017). None of the limitation scenarios resulted in a significant (> 5%) change of the free-ion concentrations of the other TM added as part of the modified Aquil media.

The cryptophyte G. cryophila (CCMP 2564), isolated from the SO, was obtained from Matt Johnson's Laboratory of Protistan Ecology at the Woods Hole Oceanography Institute, United States, while the Antarctic diatom *C. simplex* (CS 624, ANACC), isolated from the coastal waters of Antarctica (Prydz Bay), was obtained from Christel Hasslers laboratory at the University of Geneva, Switzerland. Cultures were grown at 2°C in sterile-filtered, artificial seawater medium Aquil, adjusted to the four different experimental conditions (control, -Fe, -Zn, -Co, and -B_{12}) and were exposed to 100 μmol photons m^{-2} s^{-1} on a 16:8 h light:dark cycle. Both cultures were pre-acclimated for up to 6 months to each experimental condition, during which cells counts and the photosynthetic efficiency (F_v/F_m, see below) were monitored. Both cultures were kept in mid-exponential growth by diluting them regularly with the respective media. For the main experiment, triplicate bottles for each treatment were inoculated with the corresponding pre-acclimated culture and grown until cells were in exponential growth and had reached densities of 1–1.5 $\times$ 10^5 cells mL^{-1}. An effort was made to terminate the experiments at the same time of day (10:00–14:00). Changes in cell densities were measured using a Beckman Multisizer^{TM} 3 Coulter Counter® with a 100 μm aperture. Growth rates, μ (d^{-1}), were calculated from:

$$\mu = \ln(N_t : N_0)/t$$

where N_t and N_0 are at the end and start of exponential-phase of growth, respectively and t is the time between them. Using the cell diameter obtained from the coulter counter, cell volume and surface area to volume ratios (SA/V) were calculated according to Hillebrand et al. (1999).

Determination of TM Chemistry

All labware used for analysis was pre-cleaned according to the GEOTRACES cookbook (Cutter et al., 2017). In order to minimize adsorption of TMs onto the walls of the bottle and reduce the formation of Mn and Fe hydroxides during storage, 0.2 μm pre-filtered seawater samples were acidified to pH ~1.75 with double distilled HNO$_3$ (Wuttig et al., 2019). Prior to the analysis of trace elements, the water samples along with two blanks were UV-oxidized using a 450W photochemical OV power supply (ACE GLASS Inc., Vineland, NJ, United States). During sample preparation, a buffer consisting of ammonium acetate and acetic acid was used to raise the pH to ~6 in order to promote "loss" of the trace elements onto the iminodiacetate (IDA) chelation column (Nobias, Elemental Scientific, Omaha, NE, United States) during preconcentration/matrix elimination on the SeaFAST system (Elemental Scientific, Omaha, NE, United States). Total dissolved Fe, Mn, Zn, Co, and Cu concentrations of seawater samples and the process blanks were analyzed using an online SeaFAST system (Hathorne et al., 2012),

coupled to a sector field ICP-MS (Element 2, Thermo Fisher Scientific; resolution of R = 4000). The ICP-MS was optimized daily to achieve Ba/BaO oxide forming rates below 0.3%. Each seawater sample was analyzed via standard addition, to minimize any matrix effects, which might influence the quality of the analysis. To assess the accuracy and precision of the method, a NASS-6 (National Research Council of Canada) reference standard was analyzed in a 1:10 dilution (corresponding to environmentally representative concentrations) at the beginning, in the middle and at the end of a run (two batch runs; n = 6). Recoveries for Mn, Fe, Co, Cu, and Zn were 92–101%, 88–104%, 90–100%, 88–101%, and 75–130% respectively, with no significant differences between the measured and certified values of the NASS-6.

Cellular Carbon, Nitrogen, Biogenic Silicate, and TM Quotas

Particulate organic carbon and nitrogen (POC and PON, respectively) was measured by capturing cells on pre-combusted (15 h, 500°C) GF/F filters (nominal pore size 0.7 μm; Whatman). Filters were stored at -20°C, acidified with 200 μL of 0.2N HCl and dried for > 12 h at 55°C prior to analysis on an Euro Elemental Analyzer 3000 CHNS-O (HEKAtech GmbH, Wegberg, Germany). Combusted filters were run as blanks, subtracted and POC/PON values normalized to cell densities, yielding cellular quotas. POC and PON production rates were calculated by multiplying cellular POC/PON contents by the respective growth rates. For *C. simplex*, samples for biogenic silica (BSi) were collected by gently filtering phytoplankton cells onto 0.6 μm PC filters (EMD Millipore, Darmstadt, Germany) and analyzed via a NaOH digestion procedure as described in Brzezinski and Nelson (1995). For TM contents, phytoplankton cells were collected onto 0.2 μm TM clean PC filters (EMD Millipore, Darmstadt, Germany), and rinsed for 15 min with a 0.1 M oxalic acid wash to remove trace metals bound to the cell surface (Hassler and Schoemann, 2009b). Finally, the filters were rinsed with filtered seawater and placed into TM-cleaned 25 mL polyfluor alkoxy (PFA) vials. Intracellular TM contents were subsequently analyzed via ICP-MS following a digestion with HNO$_3$ and HF (Ho et al., 2003; Twining and Baines, 2013). All filters were digested for 16 h at 180°C using 5 mL of subboiled HNO$_3$ (distilled 65%, p.a., Merck) and 0.5 mL of sub-boiled HF (40%, suprapure, Merck) followed by the addition of 0.5 mL of Milli-Q water. Under a glass hood, the volume of the cell extract was concentrated to 0.5 mL via evaporation on a 140°C hot plate and the evaporate was passed through a Ca(OH)$_2$/NaOH solution, which effectively neutralized it. 0.2 mL of subboiled HNO$_3$ (distilled 65%, p.a., Merck) was then added and the solution was transferred into 10 mL TM cleaned polypropylene (PP) vials. Finally, 10 μL of Rh (1 mg L^{-1}) was added as an internal standard and the volume was brought up to 10 mL using Milli-Q water before subsequent analysis on a high resolution ICP-MS (Attom, Nu Instruments, Wrexham, United Kingdom). Acid (5 mL of sub-boiled HNO$_3$, 0.5 mL HF) and two filter blanks as well as the BCR-414 (Plankton reference material, Sigma Aldrich, St. Louis, MO, United States) samples were also processed and analyzed in

order to assure low background TM values as well as digestion quality (**Supplementary Table 2**). Intracellular TM contents were then normalized per cell or POC.

Pigment Analysis

Analysis of pigment concentrations and photophysiological parameters for both species were conducted for the -Fe and -Zn treatments. Pigment concentrations were collected on GF/F filters, flash frozen in liquid nitrogen and stored at -80°C in the dark. Before analysis, pigments were extracted for 24 h at 4°C in the dark, using 90% acetone. Following centrifugation (5 min, 4°C, 13000 rpm) and filtrations through a 0.45 μm pore sized syringe filter, concentrations of the light harvesting (LH) pigments chlorophyll a (Chl a) and c_2 (Chl c_2), fucoxanthin (Fuco), alloxanthin (Allo) and the light protective (LP) pigments diatoxanthin (Dt), and diadinoxanthin (Dd) were determined by reverse phase high performance liquid chromatography (HPLC) on a LaChromElite® system equipped with a chilled autosampler L-2000 and a DAD detector L-2450 (VWR-Hitachi International GmbH, Darmstadt, Germany). For the separation of the pigments, a solvent gradient was applied to a Spherisorb® ODS-2 column (25 cm × 4.6 mm, 5 μm particle size; Waters, Milford, MA, United States) with a LiChropher® 100-RP-18 guard cartridge (Wright et al., 1991). Peaks were identified, quantified against known concentrations of standards for the pigments in question (DHI Lab Products, Hørsholm, Denmark) and analyzed using the EZChrom Elite (Ver. 3.1.3.; Agilent Technologies, Santa Barbara, CA, United States). Pigment contents were then normalized to filtered volume and cell densities to yield cellular quotas.

Photosynthetic Parameters

Since Zn and Fe are both important in photosynthesis, the effects of -Fe and -Zn on the photophysiology of *C. simplex* and *G. cryophila* were compared to the control with a fast repetition rate fluorometer (FRRf) in combination with a FastAct Laboratory system (FastOcean PTX), both from Chelsea Technologies Group Ltd. (West Molesey, United Kingdom). All measurements were conducted at 2°C following a 10 min dark acclimation period, assuring that all photosystem II (PSII) reaction centers were fully oxidized and non-photochemical quenching was relaxed (Petrou et al., 2014; Trimborn et al., 2019b). Excitation wavelength of the fluorometer's LED was 450 nm with an automated adjustment of the light intensity to 0.66–1.2 × 10^{22} photons m^{-2} s^{-1}. A single turnover mode with 100 flashlets saturation phase on a 2 μs pitch and 40 flashlets relaxation phase on a 40 μs pitch was used to increasingly saturate PSII. Iterative algorithms for the induction (Kolber et al., 1998) and relaxation phases (Oxborough et al., 2012) were applied to estimate minimum Chl a fluorescence (F_0) and maximum Chl a fluorescence (F_m). The apparent maximum quantum yield of photosynthesis of PSII (F_v/F_m) could then be calculated according to the equation:

$$F_v/F_m = (F_m - F_0)/F_m$$

Additionally, the time constant for electron transport at the acceptor side of PSII (τ, μs), the connectivity factor of adjacent PSII light harvesting complexes (P, dimensionless), the functional absorption cross section of PSII's photochemistry (σPSII, nm^2) and the concentration of functional PSII reaction centers, which was normalized to per cell ([RCII], amol $cell^{-1}$) were obtained using the FastPro8 software (Version 1.0.50, Kevin Oxborough, CTG Ltg.) as described by Oxborough et al. (2012).

After 10 min of dark acclimation, photosynthesis-irradiance-curves (PI-curves) were generated using 9 levels of irradiances between 0 and 1400 μmol photons m^{-2} s^{-1} with a 5 min acclimation to each light level followed by six subsequent Chl a fluorescence measurements at each light level. From these measurements, the light-adapted minimum (F′) and maximum (F_m′) fluorescence of the single turnover acquisition was estimated. The effective PSII quantum yield under ambient light (F_q′/F_m′) was derived according to the equation (F_m′ - F′)/F_m′ (Genty et al., 1989). Absolute electron transport rates (aETR, e^- $PSII^{-1}$ s^{-1}) for each light level were calculated from σ_{PSII} x [(F_q′/F_m′)/(F_v/F_m)] × E (Suggett et al., 2009; Huot and Babin, 2010; Schuback et al., 2015), where E denotes the instantaneous irradiance (photons m^{-2} s^{-1}). In addition, the resulting aETRs were multiplied by the [RCII]s, resulting in cellular ETRs (cETR; amol e^- $cell^{-1}$ s^{-1}; Koch et al., 2019). The cETRs vs. irradiance curves were then fitted according to Ralph and Gademann (2005), which takes into account possible photoinhibition, to determine the photosynthetic parameters minimum saturating irradiance (Ik), the maximum cETR (cETR$_{max}$) and the maximum light utilization efficiency (α). Following the PI-curve, the F_v/F_m was determined once more, after an additional 10 min dark acclimation, to assess potential damage to the photosystems. This parameter "yield recovery" is calculated from the ratio of F_v/F_m measured before and after the PI curve expressed as percent (Heiden et al., 2016). Non-photochemical quenching (NPQ) was calculated following the Stern-Volmer equation:

$$NPQ = F_m/F_m' - 1$$

Statistical Analysis

For the different limitation scenarios, differences in the various parameters were statistically evaluated using an one-way ANOVA followed by a Tukey's multiple-comparison test. A $p < 0.05$ was used to establish significant differences among treatments compared to the control.

RESULTS

TM Limitation of Cultures

One challenge of this study was the creation of TM-free media and the acclimation of the two phytoplankton strains to various limiting conditions (-Fe, -Zn, -Co, and -B_{12}). Total dissolved Fe, Zn, and Co concentrations in the modified Aquil, to which no addition of TMs and B_{12} were made, were low and ranged between 0.27–0.38 nmol L^{-1}, 0.44–1.51 nmol L^{-1}, and 1.56–2.88 pmol L^{-1}, respectively for the different batches

(**Supplementary Table 1**). Through successive transfers, both species were acclimated to the various TM limitation scenarios over a period of 6 months.

Cell Size, Growth Rate, and Particulate Organic Carbon/Nitrogen

The diatom *C. simplex* significantly reduced its cell volume from 31.9 ± 0.8 fL cell^{-1} in the control to 19.1 ± 2.1 fL cell^{-1} in the -Fe, a 40% reduction (**Figure 1A**). Conversely, a 20% increase in cell volume over the control was observed in the -Co treatment (38.4 ± 2.9 fL cell^{-1}; **Figure 1A**). No changes relative to the control were observed in the -Zn and -B$_{12}$ treatment (29.1 ± 0.6 and 31.0 ± 4.4 fL cell^{-1}, respectively, **Figure 1A**). Compared to the control (0.48 ± 0.03 d^{-1}), *C. simplex* reduced its growth rate by 53% in the -Fe and 64% in the -Zn to 0.23 ± 0.01 d^{-1} and 0.18 ± 0.01 d^{-1}, respectively (**Figure 1B**). Growth rates in the -Co and -B$_{12}$ treatments (0.41 ± 0.06 and 0.45 ± 0.04 d^{-1}, respectively) were also significantly lower. The – Fe resulted in a significant reduction of cell volume normalized POC quotas in *C. simplex* (238 ± 30 fg fL^{-1}) compared to the control (381 ± 28 fg fL^{-1}, **Figure 1**). In contrast -Zn, -Co, and -B$_{12}$ did not result a change of cell volume normalized POC quotas (381 ± 28, 357 ± 5, 354 ± 53, and 386 ± 52 fg fL^{-1}, respectively), compared to the control. Please note that the cellular concentrations of POC, PON, and BSi, not normalized to cell volume, follow the same trends and are shown in **Table 1**. The molar carbon to nitrogen (C:N) ratios of cells grown under -Co and -B$_{12}$ did not differ from the control (6.3 ± 0.3, 5.9 ± 0.2, and 6.2 ± 2.3 mol:mol, respectively) while cells grown in -Fe had a slightly higher C:N ratio (7.0 ± 0.2 mol:mol, **Figure 1D**). The most dramatic effect occurred in the -Zn treatment where the C:N ratio was twofold higher than the control (13.6 ± 0.5 mol:mol). Cell-volume normalized POC production rates, a function of carbon content and growth rate, were reduced in all limitation treatments relative to the control (198 ± 20 fg C fL^{-1} d^{-1}, **Figure 1E**). Highly significant decreases of 80 and 65% (59 ± 5.5 and 69 ± 5.5 fg C fL^{-1} d^{-1}) were observed for -Fe and -Zn, respectively. The -Co and -B$_{12}$ treatments also resulted in a moderately significant reduction by 20 and 31%, respectively (159 ± 15 and 137 ± 24 fg C fL^{-1} d^{-1}, respectively), compared to the control.

Similarly, *G. cryophila* was greatly affected by Fe and Zn limitation. Even though cell volumes decreased by 25% in -Fe compared to the control (310 ± 23 to 229 ± 2.9 fL cell^{-1}, respectively), -Zn did not cause a change in cell size (212 ± 17 fL cell^{-1}, **Figure 2A**). Compared to the control (0.26 ± 0.00 d^{-1}, **Figure 2B**), growth rates were > 80% lower in the -Fe and -Zn treatments (0.05 ± 0.00 d^{-1} and 0.05 ± 0.01 d^{-1}, respectively). The cell volume-normalized POC contents increased by 25% for -Fe (192 ± 4 fg fL^{-1}) and by 47% for -Zn (268 ± 28 fg fL^{-1}) compared to the control (144 ± 9 fg fL^{-1}, **Figure 2C**) along with the molar C:N ratios, which increased from 7.5 ± 0.1 mol:mol in the control to 15.2 ± 0.3 mol:mol and 20.3 ± 1.7 mol:mol in -Fe and -Zn, respectively (**Figure 2D**). Please note that the cellular concentrations of POC, PON, not normalized to cell volume, follow the same trends and are shown in **Table 1**. Cell
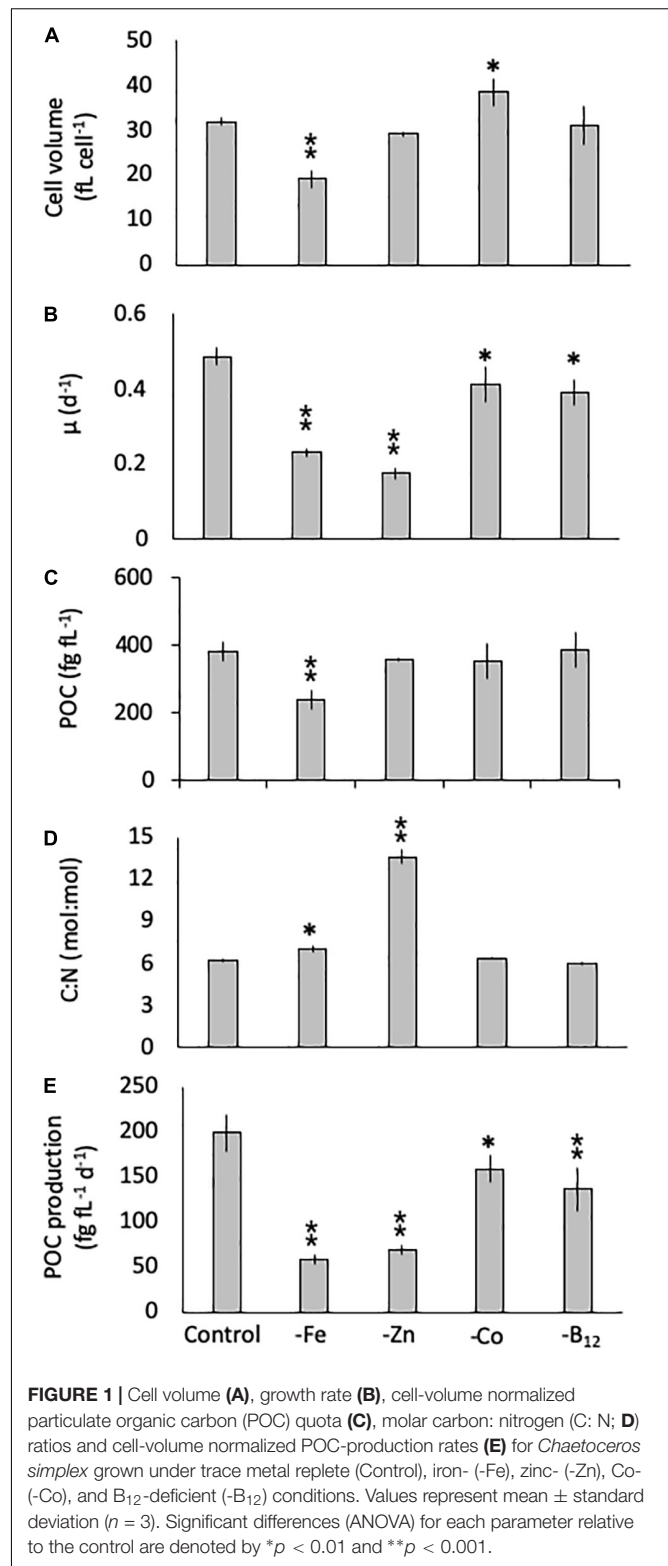

FIGURE 1 | Cell volume **(A)**, growth rate **(B)**, cell-volume normalized particulate organic carbon (POC) quota **(C)**, molar carbon: nitrogen (C: N; **D)** ratios and cell-volume normalized POC-production rates **(E)** for *Chaetoceros simplex* grown under trace metal replete (Control), iron- (-Fe), zinc- (-Zn), Co-(-Co), and B$_{12}$-deficient (-B$_{12}$) conditions. Values represent mean ± standard deviation (*n* = 3). Significant differences (ANOVA) for each parameter relative to the control are denoted by *$p < 0.01$ and **$p < 0.001$.

volume-normalized POC production rates were 44.6 ± 0.9 fg C fL^{-1} d^{-1} and 54.6 ± 17 fg C fL^{-1} d^{-1} for -Fe and -Zn, a 73 and 55% decrease over the control (121 ± 1.3 fg C fL^{-1} d^{-1}, **Figure 2E**), respectively.

TABLE 1 | Cellular carbon, nitrogen, silicon, iron, manganese, zinc, cobalt, and copper contents of *Chaetoceros simplex* and *Geminigera cryophila* grown under various TM limited regimes.

	Carbon pmol cell^{-1}	Nitrogen pmol cell^{-1}	Silicon pmol cell^{-1}	Iron amol cell^{-1}	Manganese amol cell^{-1}	Zinc amol cell^{-1}	Cobalt amol cell^{-1}	Copper amol cell^{-1}
C. simplex								
Control	1.09 ± 0.03	0.16 ± 0.01	0.12 ± 0.01	132 ± 13	170.1 ± 13.1	35.5 ± 0.2	1.05 ± 0.71	0.02 ± 0.03
-Fe	0.38 ± 0.02**	0.05 ± 0.00**	0.05 ± 0.00**	75 ± 18**	51.6 ± 2.6**	8.8 ± 4.1**	0.27 ± 0.11*	0.94 ± 0.32**
-Zn	0.87 ± 0.02**	0.06 ± 0.00**	0.07 ± 0.01**	160 ± 13*	55.0 ± 8.1**	3.1 ± 0.3**	0.40 ± 0.11	0.64 ± 0.03**
-Co	1.12 ± 0.08	0.18 ± 0.01	0.02 ± 0.00**	134 ± 32	14.5 ± 14.4**	22.9 ± 1.9**	0.09 ± 0.04**	0.22 ± 0.06**
-B12	0.99 ± 0.11	0.17 ± 0.02	0.02 ± 0.00**	76 ± 18**	10.6 ± 3.5**	23.9 ± 6.5**	0.11 ± 0.00**	0.32 ± 0.13**
G. cryophila								
Control	13.6 ± 2.10	1.43 ± 0.35	NA	571 ± 80	2.5 ± 0.5	421.0 ± 88.8	NM	NM
-Fe	17.6 ± 2.76*	1.09 ± 0.05	NA	156 ± 55*	16.6 ± 4.9**	21.9 ± 4.8**	4.9 ± 1.4	1.79 ± 0.50
-Zn	27.4 ± 4.88**	1.29 ± 0.17	NA	434 ± 191	10.9 ± 3.6**	2.6 ± 3.3**	2.2 ± 1.1	2.01 ± 1.31

*Control denotes Aquil culture media enriched with all trace metals (TM) and vitamin B$_{12}$ while -Fe, -Zn, -Co, and -B$_{12}$ stands for Aquil without Fe, Zn, Co and vitamin B$_{12}$, respectively. Values represent mean ± standard deviation (n = 3). * and** denote significant differences of p < 0.05 and p < 0.01, respectively, when compared to the control. NA, not applicable while NM, not measurable.*

Cellular Trace Metal Stoichiometry

All limitation scenarios significantly changed the carbon-normalized TM quotas of both species (expressed as μmol TM:mol C, henceforth referred to as μmol:mol). For *C. simplex,* -Fe resulted in a significant decrease in the quotas of Fe, Zn and Mn (35 ± 5.5, 28 ± 15, and 138 ± 10 μmol:mol, respectively) compared to the control (124 ± 35, 214 ± 36 and 158 ± 12 μmol:mol Fe, Zn, and Mn, respectively; **Figure 3A**). In contrast, Cu quotas increased in –Fe treatments, yielding 3.3 ± 0.4 μmol:mol compared to 2.2 ± 0.3 μmol:mol in the control treatment (**Figure 3B**) while Co remained the same (0.9 ± 0.4 and 0.6 ± 0.4 μmol:mol, respectively) in the -Fe and control treatments. The -Zn resulted in a decrease of Zn, Mn and Cu quotas (3.7 ± 0.8, 64 ± 12, and 0.6 ± 0.3 μmol:mol, respectively, **Figures 3A,B**) whereas Fe quotas (186 ± 22 μmol:mol) increased and Co quotas (0.5 ± 0.1 μmol:mol) remained similar to the control. Fe quotas remained the same in the -Co and -B$_{12}$ (115 ± 30 and 80 ± 29 μmol:mol, respectively) relative to the control treatment (124 ± 35 μmol:mol). -Co resulted in highly significant reductions in Mn, Co, Cu and Zn quotas (10.4 ± 10.3, 0.1 ± 0.0, 0.2 ± 0.1, 30 ± 39 μmol:mol, respectively), a trend mirrored in the -B$_{12}$ treatment (11 ± 2.4, 0.1 ± 0.0, 0.3 ± 0.1, 4.8 ± 2.2 μmol:mol for Mn, Co, Cu, and Zn contents, respectively) (**Figures 3A,B**).

Relative to the control treatment, *G. cryophila* also reduced its cellular TM contents when grown in -Fe and -Zn media (**Figures 4A,B**). Cellular Fe, Zn and Cu concentrations of 12.1 ± 2.9, 1.4 ± 0.5, and 0.3 ± 0.1 μmol:mol, respectively, were 75, 96, and 95% lower under -Fe than in the control treatment (49 ± 13, 37 ± 7.9, and 6.5 ± 0.5 μmol:mol, respectively, **Figures 4A,B**). In comparison the control (0.2 ± 0.2 μmol:mol), quotas of Mn (1.2 ± 0.2 μmol:mol) were similar in -Fe. -Zn resulted in a decrease of cellular Fe, Zn and Cu (0.4 ± 0.2, 0.2 ± 1, 0.2 ± 0.2 μmol:mol, respectively) relative to the control treatment while cellular Mn concentrations increased dramatically (100-fold, 30 ± 13 μmol:mol; **Figures 4A,B**). Since the values were below the detection limit, the cellular Co contents
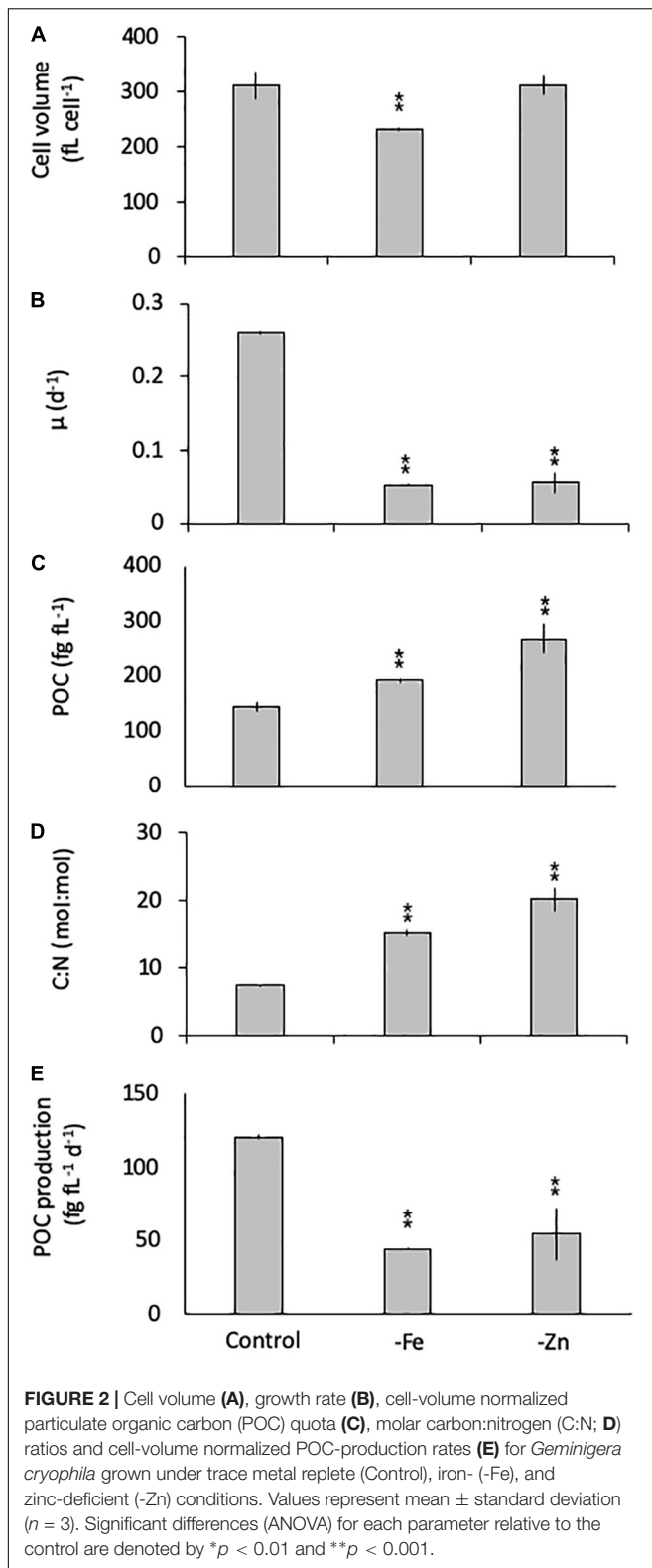
of 0.1 ± 0.0 and 0.1 ± 0.1 μmol:mol in the -Fe and -Zn treatments, respectively, could not be compared to the control. The cellular TM quotas, not normalized to cell volume, are shown in **Table 1**.

Pigments

-Fe and -Zn conditions resulted in a 78 and 74% decrease of total LH pigments in *C. simplex* (**Table 2**) compared to the control. Similarly, cellular concentrations of total LP pigments also decreased by 65 and 63% in the -Fe and -Zn treatments, respectively (**Table 2**), a trend driven primarily by a reduction of the Dd concentrations. Concentrations of LH in *G. cryophila* were significantly reduced under both, -Fe and -Zn, with a 83% decrease in the former compared to a 70% in the latter (**Table 2**).

Changes to PSII

Limitation of *C. simplex* by -Fe and -Zn significantly changed the photophysiology of PSII. F_v/F_m values, an indicator of the photosynthetic efficiency of PSII, were significantly lower in -Fe (0.19 ± 0.06) and -Zn (0.37 ± 0.02) compared to the control (0.49 ± 0.02; **Figure 5A**). Conversely -Co and -B$_{12}$ did not result in changes in F_v/F_m (data not shown) in *C. simplex*. The connectivity between adjacent photosystems P was reduced by 64 and 35% in -Fe and -Zn (0.15 ± 0.01 and 0.27 ± 0.03) compared to the control (0.42 ± 0.01; **Figure 5B**). On the other hand, σPSII, the functional absorption cross section of PSII, was significantly greater under -Fe (8.68 ± 0.59 nm^2) compared to the control (5.45 ± 0.11 nm^2) while -Zn lead to a significant decrease in σPSII (0.19 ± 0.06 nm^2; **Figure 5C**). Even though there was no significant decrease in the cellular concentration of PSII [RCII] in -Fe (0.08 ± 0.03 amol cell^{-1}), -Zn resulted in a 75% decrease (0.03 ± 0.01 amol cell^{-1}) over the control (0.13 ± 0.05 amol cell^{-1}, **Figure 5D**). Similar to F_v/F_m and P, τ, the time constant for electron transport at the acceptor side of PSII, was significantly reduced under -Fe and -Zn (498 ± 7 and 510 ± 22 μs, respectively) compared to the control (608 ± 15 μs; **Figure 5E**).

FIGURE 2 | Cell volume **(A)**, growth rate **(B)**, cell-volume normalized particulate organic carbon (POC) quota **(C)**, molar carbon:nitrogen (C:N; **D**) ratios and cell-volume normalized POC-production rates **(E)** for *Geminigera cryophila* grown under trace metal replete (Control), iron- (-Fe), and zinc-deficient (-Zn) conditions. Values represent mean ± standard deviation (n = 3). Significant differences (ANOVA) for each parameter relative to the control are denoted by *p < 0.01 and **p < 0.001.

Equally, the photophysiology of PSII in *G. cryophila* was significantly impacted by -Fe and -Zn conditions, as F_v/F_m values were reduced with 0.16 ± 0.01 and 0.37 ± 0.01, respectively,

compared to 0.44 ± 0.00 in the control (**Figure 6A**). Similarly, -Fe and -Zn led to a decrease in P (0.13 ± 0.02 and 0.20 ± 0.05) over the control (0.37 ± 0.00; **Figure 6B**). In contrast, σPSII increased significantly in –Fe and -Zn cultures (5.12 ± 0.01 and 4.93 ± 0.32 nm^2, respectively, **Figure 6C**) compared to the control (4.22 ± 0.12 nm^2). The most pronounced effects were decreases in [RCII] of 66% in the -Fe (0.61 ± 0.12 amol $cell^{-1}$) and of 93% in the -Zn (0.06 ± 0.00 amol $cell^{-1}$) compared to the control (1.80 ± 0.33 amol $cell^{-1}$; **Figure 6D**). τ was 857 ± 8 μs in the control while -Fe and -Zn conditions resulted in significantly shorter re-oxidation times (722 ± 1 and 718 ± 28 μs, respectively; **Figure 6E**).

PI Curves

PI curves for *C. simplex* resulted in similar maximum electron transport rates $cell^{-1}$ ($cETR_{max}$), half saturation constants (I_k) and α for -Fe compared to the control (**Table 3** and **Figure 7A**). Similar values were also observed in the -Zn treatment of *C. simplex* except for $cETR_{max}$, which was 32% lower compared to the control. For the diatom, the yield recovery for the -Fe and -Zn treatments were significantly lower than the control (**Table 3**). *G. cryophila* responded to -Fe and -Zn by lowering its $cETR_{max}$ $cell^{-1}$ by 17 and 94%, respectively, relative to the control (**Table 3** and **Figure 7B**). Similarly, α values were reduced by 60 and 96% under -Fe and -Zn, respectively, relative to the control. On the other hand, -Fe and -Zn resulted in significant increases in I_k relative to the control. For the cryptophyte, the yield recovery was similar for control and –Zn conditions, but was decreased in the -Fe treatment (**Table 3**). *C. simplex* increased its non-photochemical quenching (NPQ) in the control and -Zn treatments, reaching saturating levels at ∼400 μmol photons m^{-2} s^{-1} (**Figure 7C**). -Fe, however, resulted in much higher (>40%) NPQ and values did not saturate even >500 μmol photons m^{-2} s^{-1}. In contrast, *G. cryophila* increased its NPQ equally in all three treatments, with the control and -Fe saturating at ∼300 μmol photons m^{-2} s^{-1} while the -Zn cultures saturated at ∼400 μmol photons m^{-2} s^{-1} (**Figure 7D**).

DISCUSSION

Phytoplankton are important drivers of biogeochemical cycling (Hutchins and Boyd, 2016), and in the HNLC regions of the ocean, their community composition, in turn, is controlled by the availability of TMs (Sunda, 2012). Therefore, it is essential to understand how limitation by different TMs affects the physiology and elemental stoichiometry of phytoplankton. A review by Twining and Baines (2013) points out how far TM research has come since John Martin first introduced the "iron hypothesis" but it also highlights the lack of knowledge regarding the mechanisms controlling TM acquisition. Cellular concentrations of TMs have been shown to vary greatly, not just between phytoplankton groups (Twining and Baines, 2013), but also within a species (Ho et al., 2003; Sunda, 2012). Some of these variations arise from the methodological challenges of working under TM clean conditions, creating low TM media and acclimating phytoplankton to those conditions. In this study,
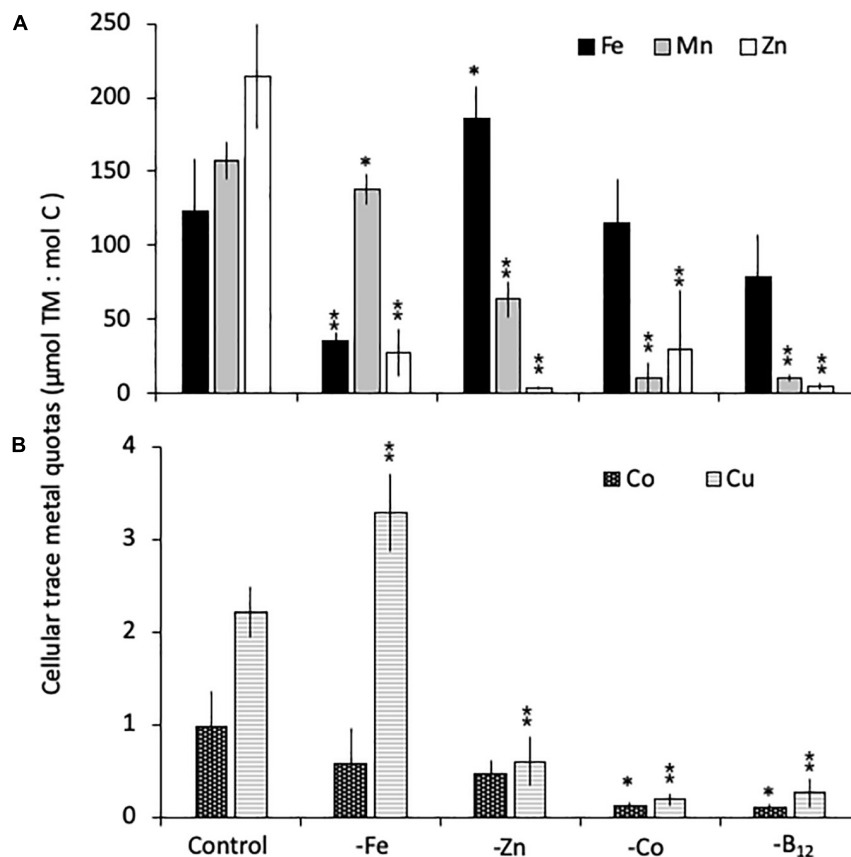
FIGURE 3 | Carbon normalized cellular quotas of the trace metals iron and zinc (Fe, Mn, and Zn, respectively; **A**), as well as copper and cobalt (Cu and Co; **B**) for *Chaetoceros simplex* grown under trace metal replete (Control), iron- (-Fe), zinc- (-Zn), Co- (-Co), and B_{12}-deficient (-B_{12}) conditions. Values represent mean ± standard deviation ($n = 3$). Significant differences (ANOVA) for each parameter relative to the control are denoted by * $p < 0.01$ and **$p < 0.001$.

prior to the addition of the TM/vitamins, TM concentrations of the modified Aquil media were 2–4 orders of magnitude lower than what is typically added with regular Aquil media (Price et al., 1989) and, except for Mn which was slightly higher, represent concentrations typical of HNLC regions of the SO (Martin et al., 1990). Irrespective of the tested TM limitation scenario (-Fe, -Zn, -Co, and -B_{12}), we observed similar physiological responses in two SO phytoplankton species of different taxonomic groups: a general decrease in growth, POC production rates and TM:C ratios. Finally, both species investigated responded to -Fe and -Zn similarly, reducing their light harvesting pigments and rearranging their thylakoid architecture to a similar degree for both scenarios. To our knowledge this represents the first data on the effects of TM limitation on the physiology of a cryptophyte species.

All TM Limitation Scenarios Resulted in Reduced Growth and POC Production Rates

Limitation by Fe and Zn drastically lowered the growth of the diatom by >50% and of the cryptophyte by > 80%. For the diatom, a more modest reduction of 20 and 15% in growth

was found for -Co and -B_{12}. Similar growth responses to B_{12} limitation have previously been described (Tang et al., 2010; Koch et al., 2013; Cruz-Lopez and Maske, 2016) and with >60% of diatoms surveyed (Tang et al., 2010) being B_{12}-auxotrophs, it is not surprising that *C. simplex* also requires this co-factor for growth. Considering the decline in growth of both species under all limitation scenarios, this clearly shows that all limitation scenarios were able to limit the growth of both species. Reductions in growth have previously been observed for -Fe (Strzepek et al., 2012; Koch et al., 2019), -Zn (Sunda and Huntsman, 1992; Saito and Goepfert, 2008), and -Co (Saito et al., 2002; Hawco and Saito, 2018). In contrast to other limitation scenarios, the reduction in growth was also accompanied by a smaller cell volume, thereby resulting in higher surface to volume ratio (S/V) for the Fe-limited cells of the two tested species. The latter is a typical adaptation of cells to low Fe environments (Raven and Kubler, 2002; Strzepek et al., 2012; Sunda, 2012), facilitating access to lower levels of TMs. In contrast and for unknown reasons, none of the two Zn-limited species altered their cell size. Co-limited cells of *C. simplex*, on the other hand, had a larger cell volume and therefore a 6% reduction of the S/V ratio, a phenomenon which was previously described for Co-starved cultures of the coccolithophorid *Emiliania huxleyi*
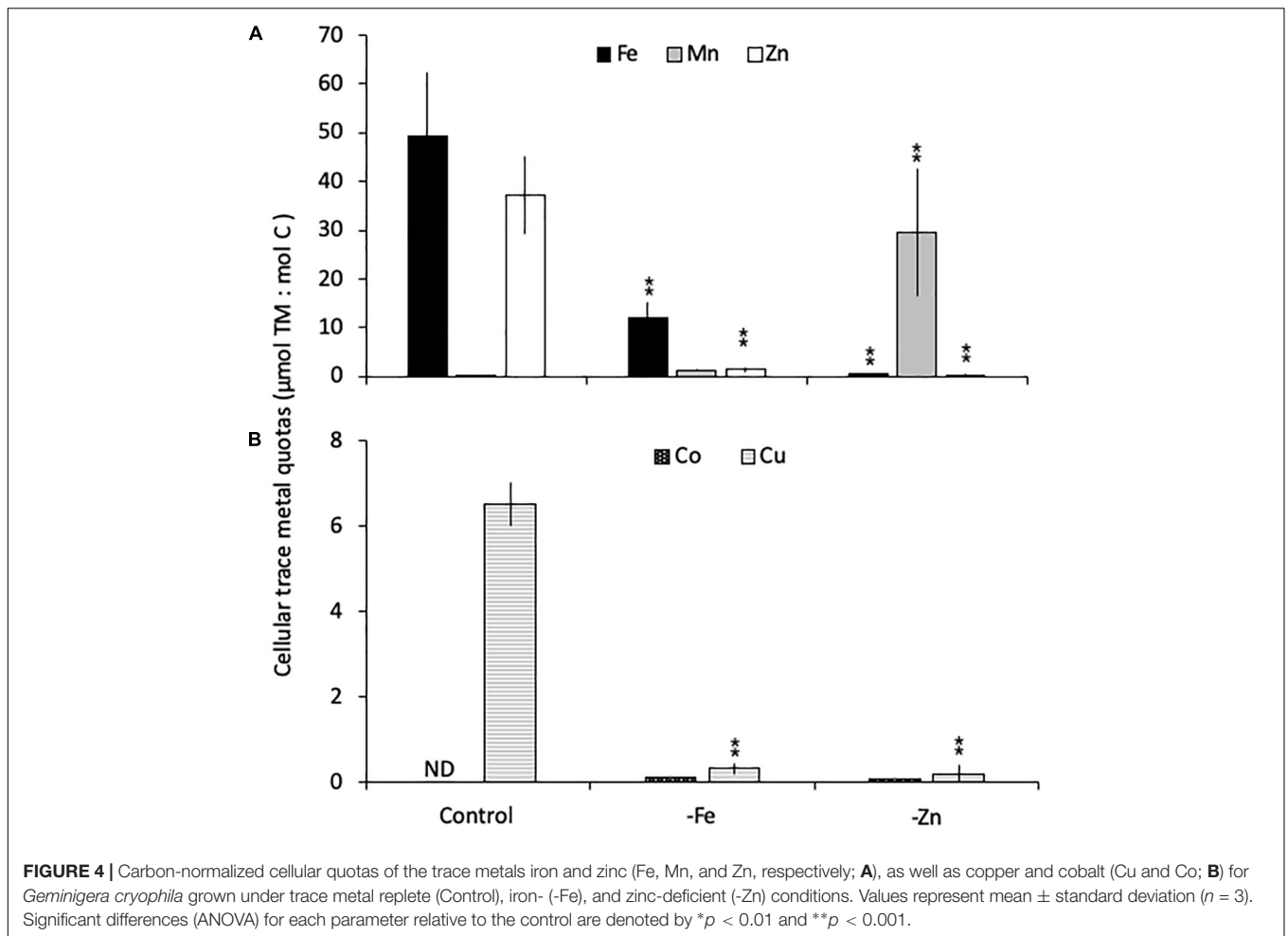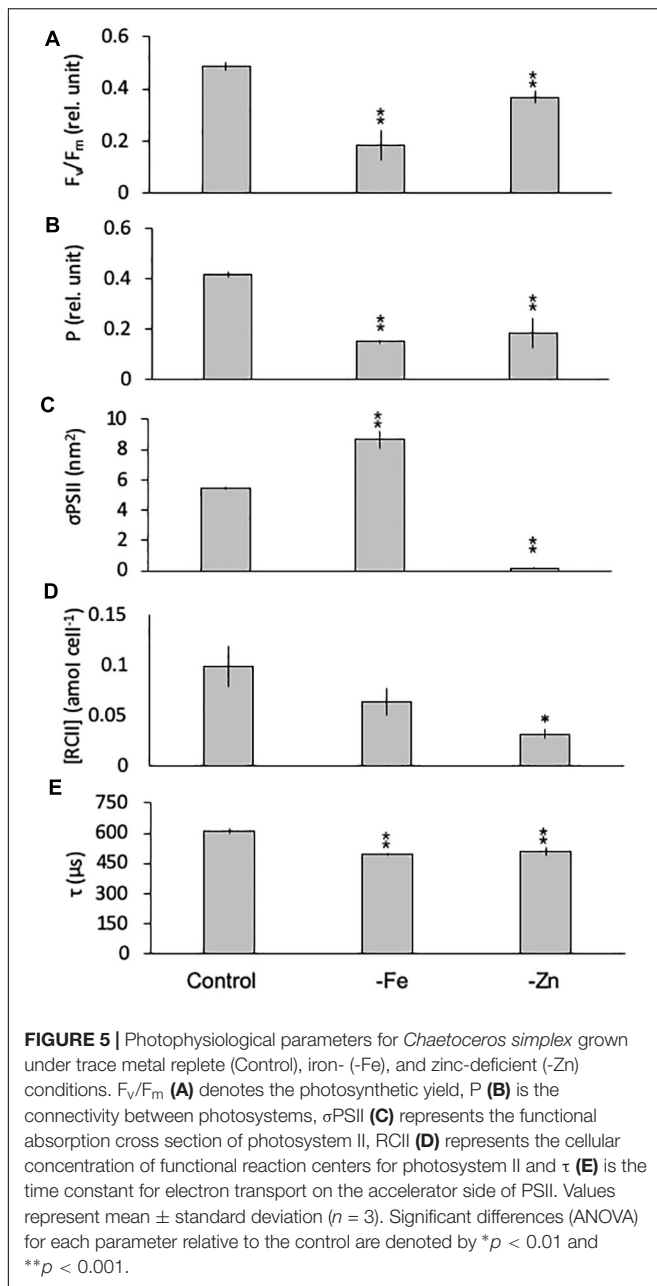
FIGURE 4 | Carbon-normalized cellular quotas of the trace metals iron and zinc (Fe, Mn, and Zn, respectively; **A**), as well as copper and cobalt (Cu and Co; **B**) for *Geminigera cryophila* grown under trace metal replete (Control), iron- (-Fe), and zinc-deficient (-Zn) conditions. Values represent mean ± standard deviation (n = 3). Significant differences (ANOVA) for each parameter relative to the control are denoted by *p < 0.01 and **p < 0.001.

TABLE 2 | Cellular concentrations of total light harvesting pigments (Total LH) including chlorophyll a (Chl a), chlorophyll c_2 (Chl c_2), fucoxanthin (Fuco), alloxanthin (Allo) and of total light protective pigments (Total LP), including diadinoxanthin (Dd) and diatoxanthin (Dt) as well as the Dt/Dd ratios for *Chaetoceros simplex* and *Geminigera cryophila* grown under trace metal replete (Control) and iron deplete (-Fe) and zinc deplete (-Zn) conditions.

Pigment	*Chaetoceros simplex*			*Geminigera cryophila*		
(fg cell^{-1})	Control	-Fe	-Zn	Control	-Fe	-Zn
Light harvesting						
Total LH	437 ± 14	96 ± 6*	114 ± 16*	3288 ± 106	882 ± 46*	1003 ± 39*
Chl a	224.2 ± 10.5	51.6 ± 4.9*	64.2 ± 14.8*	2515.2 ± 104.4	494.6 ± 83.6*	774.8 ± 14.5*
Chl c_2	13.4 ± 0.3	2.8 ± 0.1*	3.7 ± 0.1*	3.3 ± 0.1	106 ± 4.4*	–
Fuco	199 ± 10.9	41.7 ± 1.9*	46.7 ± 1.2*	671 ± 46.2	240 ± 46.2*	184 ± 32.9*
Allo	NA	NA	NA	97.9 ± 5.9	41.2 ± 1.7	43.8 ± 3.1
Light protective						
Total LP	53.8 ± 8.8	18.6 ± 1.5*	19.7 ± 1.3*	NA	NA	NA
Dd	48.0 ± 10.2	18.4 ± 1.3*	18.5 ± 1.9*	NA	NA	NA
Dt	5.8 ± 1.4	0.2 ± 0.3*	1.2 ± 0.8*	NA	NA	NA
Dt/Dd	0.13 ± 0.05	0.02 ± 0.00*	0.09 ± 0.01	NA	NA	NA

*Values represent mean ± standard deviation (n = 3). Significant changes (p < 0.05, ANOVA) in pigment concentrations relative to the controls are denoted by *. NA, not applicable.*

(Sunda and Huntsman, 1995). Similar to this study, others also describe variable responses in cell size for different species and the limiting TM investigated, with some reporting increases in cell size with -Zn (Varela et al., 2011) and -Fe (Meyerink et al., 2017) while others report no change in cell size for -Zn (Sunda and Huntsman, 1995) and B_{12} (Koch et al., 2013). In line
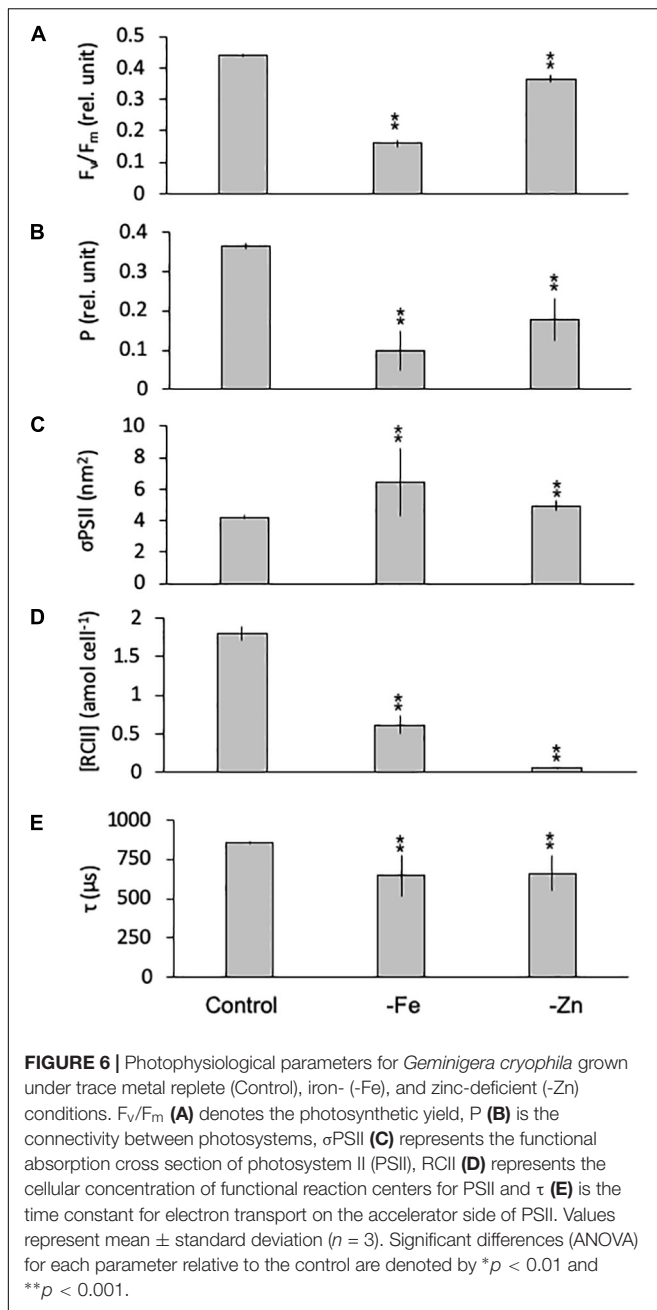
FIGURE 5 | Photophysiological parameters for *Chaetoceros simplex* grown under trace metal replete (Control), iron- (-Fe), and zinc-deficient (-Zn) conditions. F_v/F_m **(A)** denotes the photosynthetic yield, P **(B)** is the connectivity between photosystems, σPSII **(C)** represents the functional absorption cross section of photosystem II, RCII **(D)** represents the cellular concentration of functional reaction centers for photosystem II and τ **(E)** is the time constant for electron transport on the accelerator side of PSII. Values represent mean ± standard deviation (n = 3). Significant differences (ANOVA) for each parameter relative to the control are denoted by $*p < 0.01$ and $**p < 0.001$.

with this study, however, -Fe often results in a significant decrease in cell volume (Strzepek et al., 2012; Koch et al., 2019).

For the diatom, the reduction in growth rate across the treatments also resulted in significantly less POC production per cell, a fact further exacerbated in Fe-limited cells by the reduced cell volume-normalized POC quotas and cell size. Similarly, Koch et al. (2019) described that *P. antarctica* also reduced its cell size, growth rate and POC content, resulting in reduced POC production rates in response to -Fe. In contrast, *G. cryophila* increased its cell volume-normalized POC quotas by 2- and 2.5-fold for -Fe and -Zn, respectively. None the less the accompanied fivefold reduction in growth rate under -Fe and –Zn conditions suggests that cells were unable to divide

effectively, a fact which led to significantly lower POC production over the course of the experiment. Another reason for this reduced POC production may be that the Zn containing enzyme carbonic anhydrase is important for carbon acquisition in phytoplankton, and thus Zn limitation can inhibit carbon uptake (Morel et al., 1994). Even though some phytoplankton species can substitute Co for Zn (Sunda and Huntsman, 1995; Saito and Goepfert, 2008), similar to *Chaetoceros calcitrans* (Timmermans et al., 2001) neither *C. simplex* nor *G. cryophila* appear to possess this capability.

Fe plays a major role in the nitrogen metabolism of the cell. Because of its important role in the reduction of both, nitrate to nitrite and nitrite to ammonium, via the enzymes nitrate and nitrite reductase, respectively, nitrogen assimilation can be severely impacted by Fe limitation (Morel et al., 1991; Milligan and Harrison, 2000). Indeed, the drastic increase in the C:N ratio of both species under -Fe suggests that cells were either N limited or acquired excess C. Since in *C. simplex*, cell volume-based POC quotas decreased or remained the same for -Fe and -Zn, respectively, a reduced supply of new nitrogen, rather than an increase in C was likely responsible for the higher C:N ratios under both limitation scenarios. Cells can compensate for this by recycling/relocating amino acids from proteins as previously observed in Fe-starved cells of the same *P. antarctica* strain (Koch et al., 2019) and diatoms (Allen et al., 2008; Nunn et al., 2013). In line with this, less gene transcripts for nitrite and sulfur reductases in Fe-limited *P. antarctica* were reported (Koch et al., 2019). In addition the compromised photochemical efficiency of PSII (reduced F_v/F_m values) of -Fe and –Zn-limited *C. simplex* cells likely resulted in less energy equivalents being turned into PON, which, coupled to more recycling of N compounds, likely resulted in the observed increase of C:N. In contrast, *G. cryophila* increased its cell-volume normalized POC contents by ∼130 and 190% under Fe and Zn limitation, with the C:N ratio increasing by ∼20 and 300%. This finding suggests that both, the strong increase in cell-volume normalized POC buildup together with reduced assimilation of new nitrogen were responsible.

For *C. simplex*, Fe and Zn-limited cells had 55 and 35%, respectively, less silicate cell^{-1} compared to the control (**Table 1**). This was also the case when BSi was normalized to cell volume, accounting for the changes in cell size (**Supplementary Figure 1A**) and is contrary to other studies with diatoms, which have described similar (Meyerink et al., 2017) or increasing (De La Rocha et al., 2000; Leynaert et al., 2004) cellular- and volume-normalized BSi under Fe and Zn limitation. The decreased Si quotas observed here may be attributed to a direct role of Zn in the uptake and assimilation of silicate (Sinoir et al., 2012). It has been shown that the affinity of the Si transport system is Zn-dependent (De La Rocha et al., 2000) and Zn limitation resulted in significantly lower Si incorporation rates (Varela et al., 2011). All limitation scenarios had significantly lower (10–50-fold) cell- and carbon-normalized Zn quotas compared to the control suggesting that the Si metabolism of the cells may have been Zn-limited. Diatoms utilize silicate roughly 1:1 with nitrogen (Brzezinski, 1985), and while they often decrease their cell size and thus POC cell^{-1} in response to Fe- and Zn-limitation, some increase their Si content relative to C or

to N, thus raising the Si:N in the -Fe and -Zn. In contrast, neither PON nor growth rates explain the puzzling reduction of the Si:N in the -Co and -B_{12} treatments, and though we cannot explain the processes behind this phenomenon the reduced BSi quotas likely drive this trend.

Zn Limitation Affects the Photophysiology of PSII to a Much Greater Degree Than Fe Limitation

Both Zn and Fe play an important role in photosynthesis. Fe is necessary for chlorophyll synthesis and represents an integral part of the electron transport chain of respiration and photosynthesis (Raven et al., 1999; Behrenfeld and Milligan, 2013; Twining and Baines, 2013). Zn plays a role in carbonic anhydrase and is required in Cu/Zn superoxide dismutase (Alscher et al., 2002; Twining and Baines, 2013). It has been well documented that a lack of Fe results in chlorosis and a general reduction of pigments (van Leeuwe and Stefels, 1998, 2007; Koch et al., 2019). Similarly in this study, both species reduced their LH pigment quotas by >75% when Fe limited. These Fe-dependent reductions in LH pigments were compensated by an increase in σPSII, just as observed for other Fe-limited SO species (Strzepek et al., 2012; Koch et al., 2019; Trimborn et al., 2019b). Strzepek et al. (2012) described the increase in the size, rather than the number of photosynthetic units, as the adaptive strategy used to combat Fe limitation by Antarctic phytoplankton. In this study, these photophysiological adjustments (LH pigments and σPSII) were also apparent in the Zn-limited cryptophyte. The limitation of both Fe and Zn– further resulted in a significant decrease in [RCII] and connectivity (P) between PSII, thus resulting in reduced photochemical efficiency of PSIIs (F_v/F_m) for both species. A low yield, in turn, signals poor transfer of electrons from PSII to PSI, as frequently observed here and by others for cells experiencing Fe limitation (Strzepek et al., 2012; Petrou et al., 2014).

Even though cellular POC was significantly lower for *C. simplex* grown in -Fe, $cETR_{max}$ and light use efficiencies (I_k and α) were similar to the control. This suggests that although Fe-limited *C. simplex* cells were able to adjust their photophysiology, providing a similar energy supply across PSII, this energy flow was not turned into biomass and was dissipated as excess energy. Alternative electron flow likely acted as a "safety valve," keeping the primary quinone acceptor oxidized when excitation pressure on the electron chain was high and dissipating excess energy equivalents, as has been observed for other Fe-limited phytoplankton (Schuback et al., 2015; Koch et al., 2019). In Fe-limited *C. simplex*, the increase in the ratio of LP:LH pigments and NPQ suggest active heat dissipation via the xanthophyll cycle to protect the cells from excess energy, as previously observed for this strain under Fe-limitation (Petrou et al., 2014).

Even though similar to the diatom, the cryptophyte adjusted its thylakoid architecture to –Fe (reduced LH pigments, P and [RCII] compensated by larger σPSII), cellular electron transport rates and light use efficiency were, however, drastically impacted, as evident by the decrease in α coupled to the increase in I_k.

FIGURE 6 | Photophysiological parameters for *Geminigera cryophila* grown under trace metal replete (Control), iron- (-Fe), and zinc-deficient (-Zn) conditions. F_v/F_m **(A)** denotes the photosynthetic yield, P **(B)** is the connectivity between photosystems, σPSII **(C)** represents the functional absorption cross section of photosystem II (PSII), RCII **(D)** represents the cellular concentration of functional reaction centers for PSII and τ **(E)** is the time constant for electron transport on the accelerator side of PSII. Values represent mean ± standard deviation (n = 3). Significant differences (ANOVA) for each parameter relative to the control are denoted by *p < 0.01 and **p < 0.001.

N (Marchetti and Cassar, 2009). Our data shows that *C. simplex* significantly increased their Si:N ratio from 0.76 ± 0.03 in the control to 0.94 ± 0.07 and 1.15 ± 0.25 mol:mol in -Fe and -Zn, respectively (**Supplementary Figure 1B**). This was likely due to the greatly reduced PON as well as the reduction in growth rate. While nitrogen and carbon metabolic pathways are interlinked in phytoplankton, (Turpin et al., 1988; Turpin, 1991; Vergara et al., 1998) the silicate metabolism of diatoms is influenced more by the cell cycle rather than by photosynthesis (Brzezinski, 1992; Brzezinski and Conley, 1994). Thus if the cells have reduced division rates and girdle formation proceeds cell division (Claquin et al., 2002) they may acquire extra Si relative

TABLE 3 | Photophysiological parameters for *Chaetoceros simplex* and *Geminigera cryophila* grown under trace metal replete (Control), iron- (-Fe), and zinc-deplete (-Zn) conditions.

	Chaetoceros simplex			*Geminigera cryophila*		
	Control	-Fe	-Zn	Control	-Fe	-Zn
cETR$_{max}$ (e$^-$ cell^{-1} s^{-1})	44 ± 18	35 ± 15	29 ± 2*	173 ± 6	143 ± 3**	11 ± 1**
α (rel. unit)	0.21 ± 0.04	0.26 ± 0.05	0.09 ± 0.02	3.52 ± 0.33	1.19 ± 0.03**	0.12 ± 0.00**
I$_k$ (μmol photons m^{-2} s^{-1})	204 ± 64	134 ± 29	324 ± 76	49 ±15	121 ± 0*	95 ± 30*
Yield recovery (%)	65 ± 1	40 ± 5**	57 ± 4*	76 ± 6	42 ± 6	68 ± 10

cETR$_{max}$ is the maximal absolute electron transport rate (normalized to cell^{-1}) and α represents the slope of the photosynthesis irradiance (PI) curve under light limiting conditions. I$_k$ denotes the light intensity, at which electron transport is 50% of aETR$_{max}$. The yield recovery is given as a percent and represents the F$_v$/F$_m$ measured at the end of the PI curve compared to the F$_v$/F$_m$ at the beginning. Values represent mean ± standard deviation (n = 3). Significant changes (ANOVA) relative to the controls are denoted by *p < 0.01 and **p < 0.001.
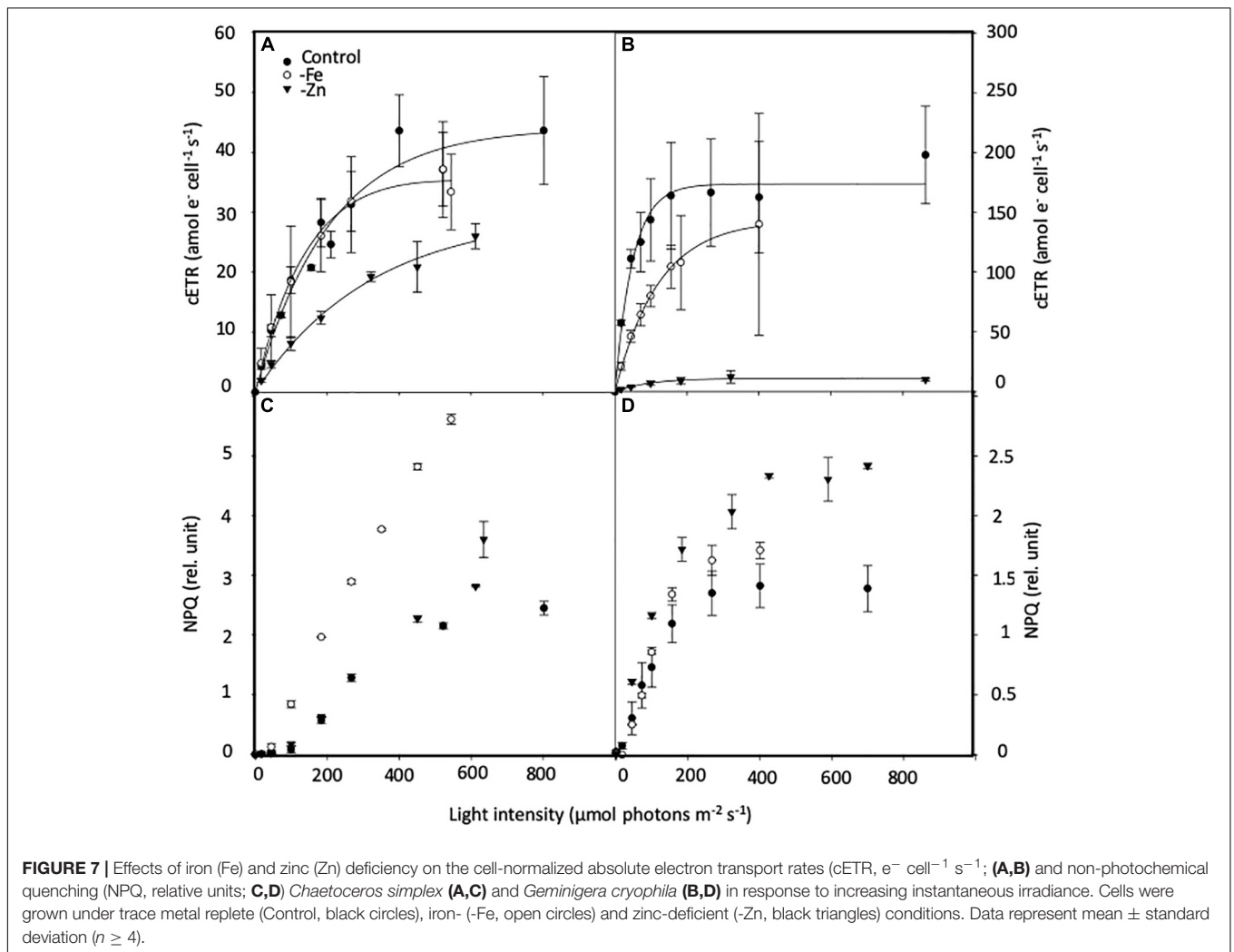
FIGURE 7 | Effects of iron (Fe) and zinc (Zn) deficiency on the cell-normalized absolute electron transport rates (cETR, e$^-$ cell^{-1} s^{-1}; **(A,B)** and non-photochemical quenching (NPQ, relative units; **C,D)** *Chaetoceros simplex* **(A,C)** and *Geminigera cryophila* **(B,D)** in response to increasing instantaneous irradiance. Cells were grown under trace metal replete (Control, black circles), iron- (-Fe, open circles) and zinc-deficient (-Zn, black triangles) conditions. Data represent mean ± standard deviation (n ≥ 4).

Surprisingly, NPQ of the –Fe-limited cells of *G. cryophila* were only slightly higher than for those in the control. Little is known about the photophysiology of cryptophytes and in particular about NPQ. Only recently, a new type of NPQ in the temperate cryptophyte *Rhodomonas salina* was found, which does not involve a light-induced xanthophyll cycle and resembles the fast and energetic quenching of higher plants (Kana et al., 2012). The

authors suggested that NPQ in this species was only induced when the Calvin cycle was saturated. Similar observations were made when *G. cryophila* was grown under increasing light levels (Trimborn et al., 2019b). In this study, NPQ was similar between control and -Fe treatments while cETRmax were significantly reduced in the Fe-limited *G. cryophila* Moreover the latter displayed, higher cell volume specific carbon content, pointing

toward an increased efficiency in linear electron transport to the Calvin cycle and therefore no further enhancement in NPQ. This increase in cellular carbon was mainly the result of the lack of cell division, resulting in the strongly reduced POC production rates observed.

Interestingly, limitation by Zn led to more drastic photophysiological adjustments of both species than by -Fe since the $cETR_{max}$ were more strongly reduced compared to the control and -Fe. While for control and –Fe conditions, *C. simplex* was able to adjust its $cETR_{max}$ to deliver the same amount of light energy through PSII, -Zn resulted in a 25% reduction of the $cETR_{max}$. This was due to the significantly smaller σPSII and much less functional PSII. Zn-limited *C. simplex* attempted to compensate for this by increasing the flow of electrons across each PSII (**Supplementary Figure 2**). Since Zn is important in carbon acquisition down the line, it is possible that -Zn and resulting carbon limitation could have resulted in a reduced demand for energy equivalents required for C-fixation. Because of this apparent reduction in energy supply, cells did not exhibit any signs of energy dissipation via the de-epoxidation of Dd to Dt, with NPQ being the same as in the control. Curiously while in -Fe limited phytoplankton the reduction in F_v/F_m is often coupled to an increase in σPSII, this was not the case for *C. simplex* in this study, something which we cannot explain. Similar to -Fe, *G. cryophila*, responded more severely to -Zn than *C. simplex* with a 97% reduction in [RCII] resulting in a dramatic decrease of $cETR_{max}$ (93%). Unlike *C. simplex,* however, -Zn led to an increase of cell volume-normalized POC, likely due to the fact that cells were not dividing. Also in -Zn, the cryptophyte increased its σPSII while also increasing NPQ over the control and -Fe. The increase of NPQ can only mean that even the severely reduced amount of energy being collected (low $cETR_{max}$) was too much, since it is accumulating in the cells, which are not dividing. Indeed an increase in NPQ for this species and another cryptophyte has been linked to downstream saturation of the Calvin cycle (Kana et al., 2012; Trimborn et al., 2019b).

The Elemental Stoichiometry Is Altered Similarly in All Limitation Scenarios

Factors which control the cellular TM content of phytoplankton are still poorly understood (Sunda, 2012). Twining and Baines (2013) suggest an ecological importance of various TMs based on their cellular concentrations in phytoplankton communities. In this study, the TMs quotas measured in the control treatments for both species are in a similar range with previous studies (Ho et al., 2003; Sunda, 2012), although cellular Zn concentrations in the former were higher. A similar pattern was observed for *P. antarctica* and led Koch et al. (2019) to speculate that the higher ambient Zn concentrations experienced by phytoplankton south of the Polar Front (Croot et al., 2011) may have resulted in the higher Zn:C ratios observed here, and also described for other SO plankton (Strzepek et al., 2011). Hassler and Schoemann (2009a) reported that the Fe:C content of four phytoplankton species, including *C. simplex* were positively correlated to their SA/V ratio. Indeed when combining the data of this study with those from Koch et al. (2019), this trend is supported

for all TMs measured, not just Fe, and supports the notion that SA/V ratio is a key determinant of the internal TM:C ratio in plankton.

All limitation scenarios resulted in a significant change of the cell- and carbon-normalized TM quotas of *C. simplex* and *G. cryophila*. With a couple of exceptions, limitation by one TM/vitamin resulted in reduced TM quotas of others, similar to observations for *P. antarctica*, where the TM quotas of all TMs, not just Fe, decreased under –Fe (Koch et al., 2019). The cellular TM quota is determined by complicated and sometimes competing mechanisms, about which, much is still unknown (Sunda, 2012). Biodilution of TMs, first described by Sunda and Huntsman (1998), for example, occurs when growth is limited by a TM (i.e., Fe), resulting in reduced cellular Fe and C compared to other TMs (i.e., Zn) who's short term uptake rates remain the same, resulting in elevated Zn:C in Fe limited plankton. Sunda and Huntsman (2004) and Lane et al. (2009) describe this process in -Fe cultures of *Thalassiosira pseudonana* and *P. antarctica* for Zn:C and Cd:C ratios, respectively. In this study the only increases of TM:C observed were in Cu:C in *C. simplex* in -Fe and in Mn:C in *G. cryophila* in -Zn, suggesting that, just like for *P. antarctica* (Koch et al., 2019) and other SO phytoplankton (Strzepek et al., 2012), biodilution is not the main determinant of TM:C quotas here. It is worth mentioning that in the latter studies, cellular TM quotas were directly measured via ICP-MS once cells have reached sufficient densities, while in the former studies, quotas were calculated from short term uptake experiments. A comparison of the two approaches is presented in King et al. (2012).

As reported for other diatoms (Annett et al., 2008), we observed an increase in Cu:C for *C. simplex* grown in -Fe. Cu is an important redox element, in freshwater green algae, higher plants and some phytoplankton, where it is required for plastocyanin, the main electron carrier from the cytochrome b6f complex of PSII to PSI (Raven et al., 1999; Behrenfeld and Milligan, 2013). Even though most diatoms use Fe containing cytochrome c_6, some open ocean species were identified to use plastocyanin in order to alleviate Fe deficiency (Peers and Price, 2006). The elevated Mn:C ratio of Zn-limited *G. cryophila* on the other hand, may be a response to a secondary Fe limitation. Mn is needed in superoxide dismutases (SOD), antioxidants important in combating reactive oxygen species (ROS). Similar to what has been observed by Peers and Price (2004), the increase in Mn:C could be due to a switch from Fe-SOD to Mn-SOD in *G. cryophila* caused by the low Fe:C in the -Zn.

Substitution of one TM for another may be another mechanism controlling the cellular TM quotas in phytoplankton. This has been demonstrated for *P. antarctica* (Saito and Goepfert, 2008), *Emiliania huxleyi* (Xu et al., 2007), and *Thalassiosira weissflogii* (Lee and Morel, 1995) which were able to exchange Zn, Co, and Cd to varying degrees. While we cannot rule out that in *C. simplex*, Co limitation may have been alleviated by Zn, as evident by the higher growth rates in the -Co compared to the -Zn, there are not many reported cellular functions for Co, other than as substitute for Zn or production of B_{12} in prokaryotes (Saito et al., 2002; Twining and Baines, 2013). Also, not all phytoplankton species seem to have the ability to substitute one TM for another. Experiments conducted with

another *Chaeotceros* species revealed that, just like *C. simplex*, *C. calcitrans* was not able to alleviate Zn limitation by substituting Co (Timmermans et al., 2001).

The TM:C in the -Co and -B$_{12}$ were amongst the lowest measured of all the treatments. A similar reduction in the Co:P, Zn:P, and Cd:P ratios were observed for B$_{12}$-limited *Attheya* sp., while, like in this study, the Fe:P remained unchanged (King et al., 2011). Co-limitation of phytoplankton by Fe and B$_{12}$ has previously been observed in the HNLC regions of the North Pacific (Koch et al., 2011; Cohen et al., 2017) and Southern Ocean (Panzeca et al., 2006; Bertrand et al., 2007), and along the eastern boundary of the South Atlantic gyre (Browning et al., 2017), hinting at the important potential interaction of these two micronutrients. This study is one of only two (King et al., 2011) describing the effects of B$_{12}$ limitation on the cellular TM stoichiometry and warrants more research. Also it is worth pointing out that just like the reduced TM:C ratios (Mn, Zn, Co, and Cu) for *C. simplex*, the Si:N ratios were also lowest in the -Co and -B$_{12}$ treatments. Indeed, Zn and Fe, are not only important in the silicification process (Sinoir et al., 2012; Meyerink et al., 2017), but are integrated into the diatom frustules themselves (Jaccard et al., 2009; Ingall et al., 2013). Thus, while maintaining a similar C:N, the decrease of Si:N could have caused the much lower TM:C observed in the -Co and -B$_{12}$ treatments.

CONCLUSION

Observations that TMs can be exchanged and that the uptake of one can compete and even inhibit another, suggest that the underlying mechanisms of TM acquisition are similar. This is consistent with our results, which show similar cellular TM:C ratios under most tested TM scenarios. Furthermore, Koch et al. (2019), described a fourfold reduction of genes encoding for a Zn and mitochondrial metal ion transporter in Fe-limited *P. antarctica*, consistent with the lower TM:C (Fe, Mn Zn, Co, Cu) ratios observed. If in the culture media only one TM is less abundant, and the metal quotas of phytoplankton are governed by the cellular requirements for each metal, as assumed under Redfield, the scarcity of this one TM should not necessarily result in a lower cellular content of all other TMs, as has been observed here and by Koch et al. (2019). These observations suggest that a consequence of limitation by one TM may be a secondary and perhaps more fatal limitation by another and fits with Saito et al. (2008) definition of Type III colimitation. Thus the observed -Fe effects on the physiology, for example, may in actuality be the result of Zn limitation, brought on by the lower Zn:C ratios resulting from low Fe. Undoubtedly in vast regions of the world's ocean Fe is limiting primary production, as has been established

by a number of large scale ocean Fe-fertilization studies and several shipboard incubations (see de Baar et al., 2005). But as this study shows, the physiological responses to limitation by two TMs can be very similar even across phytoplankton taxa, and thus it may be difficult to identify the limiting TM by looking simply at certain proxies such as the photosynthetic yield (F$_v$/F$_m$). From this viewpoint, phytoplankton taxa in HNLC regions are not only selected by their ability to adapt to Fe stress, but also how well they can cope with low cellular concentrations of other TMs. Additionally the phenomenon of reduced cellular quotas of other TMs due to Fe limitation must be considered when constructing global biogeochemical models.

DATA AVAILABILITY

All datasets generated for this study are included in the manuscript and/or the **Supplementary Files**.

AUTHOR CONTRIBUTIONS

FK conceptualized and conducted the experiments. FK and ST wrote the manuscript.

FUNDING

ACKNOWLEDGMENTS

SUPPLEMENTARY MATERIAL

The Supplementary Material for this article can be found online at: https://www.frontiersin.org/articles/10.3389/fmars.2019.00514/full#supplementary-material

REFERENCES

Allen, A. E., LaRoche, J., Maheswari, U., Lommer, M., Schauer, N., Lopez, P. J., et al. (2008). Whole-cell response of the pennate diatom *Phaeodactylum tricornutum* to iron starvation. *Proc. Natl. Acad. Sci. U.S.A.* 105, 10438–10443. doi: 10.1073/pnas.0711370105

Alscher, R. G., Erturk, N., and Heath, L. S. (2002). Role of superoxide dismutases (SODs) in controlling oxidative stress in plants. *J. Exp. Bot.* 53, 1331–1341. doi: 10.1093/jexbot/53.372.1331

Annett, A. L., Lapi, S., Ruth, T. J., and Maldonado, M. T. (2008). The effects of Cu and Fe availability on the growth and Cu: C ratios of marine diatoms. *Limnol. Oceanogr.* 53, 2451–2461. doi: 10.4319/lo.2008.53.6.2451

Banerjee, R., and Ragsdale, S. W. (2003). The many faces of vitamin B-12: catalysis by cobalamin-dependent enzymes. *Annu. Rev. Biochem.* 72, 209–247. doi: 10.1146/annurev.biochem.72.121801.161828

Behrenfeld, M. J., and Milligan, A. J. (2013). "Photophysiological Expressions of Iron Stress in Phytoplankton," in *Annual Review of Marine Science*, Vol. 5, eds C. A. Carlson and S. J. Giovannoni (Palo Alto, CA: Annual Reviews), 217–246. doi: 10.1146/annurev-marine-121211-172356

Bertrand, E. M., Allen, A. E., Dupont, C. L., Norden-Krichmar, T. M., Bai, J., Valas, R. E., et al. (2012). Influence of cobalamin scarcity on diatom molecular physiology and identification of a cobalamin acquisition protein. *Proc. Natl. Acad. Sci. U.S.A.* 109, E1762–E1771. doi: 10.1073/pnas.1201731109

Bertrand, E. M., McCrow, J. P., Moustafa, A., Zheng, H., McQuaid, J. B., Delmont, T. O., et al. (2015). Phytoplankton-bacterial interactions mediate micronutrient colimitation at the coastal Antarctic sea ice edge. *Proc. Natl. Acad. Sci. U.S.A.* 112, 9938–9943. doi: 10.1073/pnas.1501615112

Bertrand, E. M., Saito, M. A., Rose, J. M., Riesselman, C. R., Lohan, M. C., Noble, A. E., et al. (2007). Vitamin B-12 and iron colimitation of phytoplankton growth in the Ross Sea. *Limnol. Oceanogr.* 52, 1079–1093. doi: 10.3389/fmicb.2011.00160

Blanco-Ameijeiras, S., Moisset, S. A. M., Trimborn, S., Campbell, D. A., Heiden, J. P., and Hassler, C. S. (2018). Elemental stoichiometry and photophysiology regulation of synechococcus sp PCC7002 under increasing severity of chronic iron limitation. *Plant Cell Physiol.* 59, 1803–1816. doi: 10.1093/pcp/pcy097

Botebol, H., Lelandais, G., Six, C., Lesuisse, E., Meng, A., Bittner, L., et al. (2017). Acclimation of a low iron adapted Ostreococcus strain to iron limitation through cell biomass lowering. *Sci. Rep.* 7:327. doi: 10.1038/s41598-017-00216-6

Browning, T. J., Achterberg, E. P., Rapp, I., Engel, A., Bertrand, E. M., Tagliabue, A., et al. (2017). Nutrient co-limitation at the boundary of an oceanic gyre. *Nature* 551, 242–246. doi: 10.1038/nature24063

Browning, T. J., Bouman, H. A., Henderson, G. M., Mather, T. A., Pyle, D. M., Schlosser, C., et al. (2014). Strong responses of Southern Ocean phytoplankton communities to volcanic ash. *Geophys. Res. Lett.* 41, 2851–2857. doi: 10.1002/2014gl059364

Brzezinski, M. A. (1985). The Si-C-N ratio of marine diatoms - interspecific variability and effect of some environmental variables. *J. Phycol.* 21, 347–357. doi: 10.1111/j.0022-3646.1985.00347.x

Brzezinski, M. A. (1992). Cell-cycle effects on the kinetics of silicic acid uptake and resource competition among diatoms. *J. Plankton Res.* 14, 1511–1539. doi: 10.1093/plankt/14.11.1511

Brzezinski, M. A., and Conley, D. J. (1994). Silicon deposition during the cell-cycle of *Thalassiosira weissflogii* (Bacillariophyceae) determined using dual rhodamine 123 and propidium iodide staining. *J. Phycol.* 30, 45–55. doi: 10.1111/j.0022-3646.1994.00045.x

Brzezinski, M. A., and Nelson, D. M. (1995). The annual silica cycle in the Sargasso Sea near Bermuda. *Deep Sea Res. Part I Oceanogr. Res. Papers* 42, 1215–1237. doi: 10.1016/0967-0637(95)93592-3

Claquin, P., Martin-Jézéquel, V., Kromkamp, J. C., Veldhuis, M. J. W., and Kraay, G. W. (2002). Uncoupling of silicon compared with carbon and nitrogen metabolisms and the role of the cell cycle in continuous cultures of *Thalassiosira pseudonana* (Bacillariophyceae) under light, nitrogen, and phosphorus control. *J. Phycol.* 38, 922–930. doi: 10.1046/j.1529-8817.2002.t01-1-01220.x

Coale, K. H. (1991). Effects of iron, manganese, copper and zinc enrichments on productivity and biomass in the sub-Arctic Pacific. *Limnol. Oceanogr.* 36, 1851–1864. doi: 10.4319/lo.1991.36.8.1851

Cohen, N. R., Ellis, K. A., Burns, W. G., Lampe, R. H., Schuback, N., Johnson, Z., et al. (2017). Iron and vitamin interactions in marine diatom isolates and natural assemblages of the Northeast Pacific Ocean. *Limnol. Oceanogr.* 62, 2076–2096. doi: 10.1002/lno.10552

Conway, T. M., Hoffmann, L. J., Breitbarth, E., Strzepek, R. F., and Wolff, E. W. (2016). The growth response of two diatom species to atmospheric dust from the last glacial maximum. *Plos One* 11:23. doi: 10.1371/journal.pone.0158553

Crawford, D. W., Lipsen, M. S., Purdie, D. A., Lohan, M. C., Statham, P. J., Whitney, F. A., et al. (2003). Influence of zinc and iron enrichments on phytoplankton growth in the northeastern subarctic Pacific. *Limnol. Oceanogr.* 48, 1583–1600. doi: 10.4319/lo.2003.48.4.1583

Croft, M. T., Warren, M. J., and Smith, A. G. (2006). Algae need their vitamins. *Eukaryot. Cell* 5, 1175–1183. doi: 10.1128/ec.00097-6

Croot, P. L., Baars, O., and Streu, P. (2011). The distribution of dissolved zinc in the Atlantic sector of the Southern Ocean. *Deep Sea Res. Part 2 Top. Stud. Oceanogr.* 58, 2707–2719. doi: 10.1016/j.dsr2.2010.10.041

Cruz-Lopez, R., and Maske, H. (2016). The Vitamin B-1 and B-12 required by the marine dinoflagellate lingulodinium polyedrum can be provided by its associated bacterial community in culture. *Front. Microbiol.* 7:13. doi: 10.3389/fmicb.2016.00560

Cutter, G., Casciotti, K., Croot, P., Geibert, W., Heimbürger, L.-E., Lohan, M., et al. (2017). *Sampling and Sample-handling Protocols for GEOTRACES Cruises*. Toulouse: GEOTRACES International Project Office.

de Baar, H. J. W., Boyd, P. W., Coale, K. H., Landry, M. R., Tsuda, A., Assmy, P., et al. (2005). Synthesis of iron fertilization experiments: from the iron age in the age of enlightenment. *J. Geophys. Res. Oceans* 110, 1–24. doi: 10.1029/2004jc002601

De La Rocha, C. L., Hutchins, D. A., Brzezinski, M. A., and Zhang, Y. H. (2000). Effects of iron and zinc deficiency on elemental composition and silica production by diatoms. *Mar. Ecol. Prog. Ser.* 195, 71–79. doi: 10.3354/meps195071

Dyhrman, S. T., and Ruttenberg, K. C. (2006). Presence and regulation of alkaline phosphatase activity in eukaryotic phytoplankton from the coastal ocean: implications for dissolved organic phosphorus remineralization. *Limnol. Oceanogr.* 51, 1381–1390. doi: 10.4319/lo.2006.51.3.1381

Genty, B., Briantais, J. M., and Baker, N. R. (1989). The relationship between the quantum yield of photosynthetic electron-transport and quenching of chlorophyll fluorescence. *Biochim. Biophys. Acta* 990, 87–92. doi: 10.1016/s0304-4165(89)80016-9

Hassler, C. S., and Schoemann, V. (2009a). Bioavailability of organically bound Fe to model phytoplankton of the Southern Ocean. *Biogeosciences* 6, 2281–2296. doi: 10.5194/bg-6-2281-2009

Hassler, C. S., and Schoemann, V. (2009b). Discriminating between intra- and extracellular metals using chemical extractions: an update on the case of iron. *Limnol. Oceanogr. Methods* 7, 479–489. doi: 10.4319/lom.2009.7.479

Hassler, C. S., Schoemann, V., Boye, M., Tagliabue, A., Rozmarynowycz, M., and McKay, R. M. L. (2012). "Iron bioavailability in the Southern Ocean," in *Oceanography and Marine Biology: An Annual Review*, Vol. 50, eds R. N. Gibson, R. J. A. Atkinson, J. D. M. Gordon, and R. N. Hughes (Boca Raton, FL: CRC Press-Taylor & Francis Group), 1–63.

Hathorne, E. C., Haley, B., Stichel, T., Grasse, P., Zieringer, M., and Frank, M. (2012). Online preconcentration ICP-MS analysis of rare earth elements in seawater. *Geochem. Geophys. Geosyst.* 13:12. doi: 10.1029/2011gc003907

Hawco, N. J., and Saito, M. A. (2018). Competitive inhibition of cobalt uptake by zinc and manganese in a pacific *Prochlorococcus* strain: insights into metal homeostasis in a streamlined oligotrophic cyanobacterium. *Limnol. Oceanogr.* 63, 2229–2249. doi: 10.1002/lno.10935

Heal, K. R., Qin, W., Ribalet, F., Bertagnolli, A. D., Coyote-Maestas, W., Hmelo, L. R., et al. (2017). Two distinct pools of B-12 analogs reveal community interdependencies in the ocean. *Proc. Natl. Acad. Sci. U.S.A.* 114, 364–369. doi: 10.1073/pnas.1608462114

Heiden, J. P., Bischof, K., and Trimborn, S. (2016). Light intensity modulates the response of two antarctic diatomspecies to ocean acidification. *Front. Mar. Sci.* 3:260. doi: 10.3389/fmars.2016.00260

Hillebrand, H., Durselen, C. D., Kirschtel, D., Pollingher, U., and Zohary, T. (1999). Biovolume calculation for pelagic and benthic microalgae. *J. Phycol.* 35, 403–424. doi: 10.1046/j.1529-8817.1999.3520403.x

Ho, T. Y., Quigg, A., Finkel, Z. V., Milligan, A. J., Wyman, K., Falkowski, P. G., et al. (2003). The elemental composition of some marine phytoplankton. *J. Phycol.* 39, 1145–1159. doi: 10.1111/j.0022-3646.2003.03-090.x

Huot, Y., and Babin, M. (2010). "Overview of Fluorescence Protocols: Theory, Basic Concepts, and Practice," in *Chlorophyll a Fluorescence in Aquatic Sciences: Methods and Applications*, eds D. J. Suggett, M. A. Borowitzka, and O. Prášil (Dordrecht: Springer).

Hutchins, D. A., and Boyd, P. W. (2016). Marine phytoplankton and the changing ocean iron cycle. *Nat. Clim. Change* 6, 1072–1079. doi: 10.1038/nclimate3147

Ingall, E. D., Diaz, J. M., Longo, A. F., Oakes, M., Finney, L., Vogt, S., et al. (2013). Role of biogenic silica in the removal of iron from the Antarctic seas. *Nat. Commun.* 4:6. doi: 10.1038/ncomms2981

Jaccard, T., Ariztegui, D., and Wilkinson, K. J. (2009). Incorporation of zinc into the frustule of the freshwater diatom Stephanodiscus hantzschii. *Chem. Geol.* 265, 381–386. doi: 10.1016/j.chemgeo.2009.04.016

Kana, R., Kotabova, E., Sobotka, R., and Prasil, O. (2012). Non-photochemical quenching in cryptophyte alga rhodomonas salina is located in chlorophyll a/c antennae. *Plos One* 7:12. doi: 10.1371/journal.pone.0029700

King, A. L., Sanudo-Wilhelmy, S. A., Boyd, P. W., Twining, B. S., Wilhelm, S., Breene, C., et al. (2012). A comparison of biogenic iron quotas during a diatom spring bloom using multiple approaches. *Biogeosciences* 9, 667–687. doi: 10.5194/bgd-8-9381-2011

King, A. L., Sanudo-Wilhelmy, S. A., Leblanc, K., Hutchins, D. A., and Fu, F. X. (2011). CO2 and vitamin B-12 interactions determine bioactive trace metal requirements of a subarctic Pacific diatom. *ISME J.* 5, 1388–1396. doi: 10.1038/ismej.2010.211

Klug, A. (2010). "The discovery of zinc fingers and their applications in gene regulation and genome manipulation," in *Annual Review of Biochemistry*, Vol. 79, eds R. D. Kornberg, C. R. H. Raetz, J. E. Rothman, and J. W. Thorner (Palo Alto, CA: Annual Reviews), 213–231. doi: 10.1146/annurev-biochem-010909-095056

Koch, F., Beszteri, S., Harms, L., and Trimborn, S. (2019). The impacts of iron limitation and ocean acidification on the cellular stoichiometry, photophysiology, and transcriptome of Phaeocystis antarctica. *Limnol. Oceanogr.* 64, 357–375. doi: 10.1002/lno.11045

Koch, F., Marcoval, M. A., Panzeca, C., Bruland, K. W., Sanudo-Wilhelmy, S. A., and Gobler, C. J. (2011). The effect of vitamin B-12 on phytoplankton growth and community structure in the Gulf of Alaska. *Limnol. Oceanogr.* 56, 1023–1034. doi: 10.4319/lo.2011.56.3.1023

Koch, F., Sanudo-Wilhelmy, S. A., Fisher, N. S., and Gobler, C. J. (2013). The effects of vitamins B1 and B12 on the bloom dynamics of the harmful brown tide alga, *Aureococcus anophagefferens* (Pelagophyceae). *Limnol. Oceanogr.* 58, 1761–1774. doi: 10.4319/lo.2013.58.5.0000

Kolber, Z. S., Prasil, O., and Falkowski, P. G. (1998). Measurements of variable chlorophyll fluorescence using fast repetition rate techniques: defining methodology and experimental protocols. *Biochim. Biophys. Acta Bioenerget.* 1367, 88–106. doi: 10.1016/s0005-2728(98)00135-2

Lane, E. S., Semeniuk, D. M., Strzepek, R. F., Cullen, J. T., and Maldonado, M. T. (2009). Effects of iron limitation on intracellular cadmium of cultured phytoplankton: implications for surface dissolved cadmium to phosphate ratios. *Mar. Chem.* 115, 155–162. doi: 10.1016/j.marchem.2009.07.008

Lee, J. G., and Morel, F. M. M. (1995). Replacement of zinc by cadmium in marine-phytoplankton. *Mar. Ecol. Prog. Ser.* 127, 305–309. doi: 10.3354/meps127305

Leynaert, A., Bucciarelli, E., Claquin, P., Dugdale, R. C., Martin-Jezequel, V., Pondaven, P., et al. (2004). Effect of iron deficiency on diatom cell size and silicic acid uptake kinetics. *Limnol. Oceanogr.* 49, 1134–1143. doi: 10.4319/lo.2004.49.4.1134

Lionetto, M. G., Caricato, R., Giordano, M. E., and Schettino, T. (2016). The complex relationship between metals and carbonic anhydrase: new insights and perspectives. *Int. J. Mol. Sci.* 17:127. doi: 10.3390/ijms17010127

Marchetti, A., and Cassar, N. (2009). Diatom elemental and morphological changes in response to iron limitation: a brief review with potential paleoceanographic applications. *Geobiology* 7, 419–431. doi: 10.1111/j.1472-4669.2009.00207.x

Martin, J. H., Gordon, R. M., Fitzwater, S., and Broenkow, W. W. (1989). VERTEX - Phytoplankton iron studies in the Gulf of Alaska. *Deep Sea Res. Part A Oceanogr. Res. Papers* 36, 649–680. doi: 10.1016/0198-0149(89)90144-1

Martin, J. H., Gordon, R. M., and Fitzwater, S. E. (1990). Iron in Antarctic waters. *Nature* 345, 156–158. doi: 10.1038/345156a0

Meyerink, S. W., Ellwood, M. J., Maher, W. A., Price, G. D., and Strzepek, R. F. (2017). Effects of iron limitation on silicon uptake kinetics and elemental stoichiometry in two Southern Ocean diatoms, Eucampia antarctica and Proboscia inermis, and the temperate diatom *Thalassiosira pseudonana*. *Limnol. Oceanogr.* 62, 2445–2462. doi: 10.1002/lno.10578

Milligan, A. J., and Harrison, P. J. (2000). Effects of non-steady-state iron limitation on nitrogen assimilatory enzymes in the marine diatom *Thalassiosira weissflogii* (Bacillariophyceae). *J. Phycol.* 36, 78–86. doi: 10.1046/j.1529-8817.2000.99013.x

Moore, C. M., Mills, M. M., Arrigo, K. R., Berman-Frank, I., Bopp, L., Boyd, P. W., et al. (2013). Processes and patterns of oceanic nutrient limitation. *Nat. Geosci.* 6, 701–710. doi: 10.1038/ngeo1765

Morel, F. M. M., Hudson, R. J. M., and Price, N. M. (1991). Limitation of productivity by trace-metals in the sea. *Limnol. Oceanogr.* 36, 1742–1755. doi: 10.4319/lo.1991.36.8.1742

Morel, F. M. M., Reinfelder, J. R., Roberts, S. B., Chamberlain, C. P., Lee, J. G., and Yee, D. (1994). Zinc and carbon co-limitation of marine-phytoplankton. *Nature* 369, 740–742. doi: 10.1038/369740a0

Nunn, B. L., Faux, J. F., Hippmann, A. A., Maldonado, M. T., Harvey, H. R., Goodlett, D. R., et al. (2013). Diatom proteomics reveals unique acclimation strategies to mitigate Fe limitation. *Plos One* 8:e75653. doi: 10.1371/journal.pone.0075653

Oxborough, K., Moore, C. M., Suggett, D. J., Lawson, T., Chan, H. G., and Geider, R. J. (2012). Direct estimation of functional PSII reaction center concentration and PSII electron flux on a volume basis: a new approach to the analysis of Fast Repetition Rate fluorometry (FRRf) data. *Limnol. Oceanogr. Methods* 10, 142–154. doi: 10.4319/lom.2012.10.142

Panzeca, C., Beck, A. J., Leblanc, K., Taylor, G. T., Hutchins, D. A., and Sanudo-Wilhelmy, S. A. (2008). Potential cobalt limitation of vitamin B-12 synthesis in the North Atlantic Ocean. *Glob. Biogeochem. Cycles* 22:7. doi: 10.1029/2007gb003124

Panzeca, C., Beck, A. J., Tovar-Sanchez, A., Segovia-Zavala, J., Taylor, G. T., Gobler, C. J., et al. (2009). Distributions of dissolved vitamin B-12 and Co in coastal and open-ocean environments. *Estuar. Coast. Shelf Sci.* 85, 223–230. doi: 10.1016/j.ecss.2009.08.016

Panzeca, C. A., Tovar-Sanchez, A., Agusti, S., Reche, I., Duarte, C. M., Taylor, G. T., et al. (2006). B Vitamins as regulators of phytoplankton dynamics. *EOS* 87, 593–596.

Peers, G., and Price, N. M. (2004). A role for manganese in superoxide dismutases and growth of iron-deficient diatoms. *Limnol. Oceanogr.* 49, 1774–1783. doi: 10.4319/lo.2004.49.5.1774

Peers, G., and Price, N. M. (2006). Copper-containing plastocyanin used for electron transport by an oceanic diatom. *Nature* 441, 341–344. doi: 10.1038/nature04630

Petrou, K., Trimborn, S., Rost, B., Ralph, P. J., and Hassler, C. S. (2014). The impact of iron limitation on the physiology of the Antarctic diatom Chaetoceros simplex. *Mar. Biol.* 161, 925–937. doi: 10.1007/s00227-014-2392-z

Price, N., Harrison, G. I., Hering, J. G., Hudson, R. J., Nirel, P. M. V., Palenik, B., et al. (1989). Preparation and chemistry of the artificial algal culture medium Aquil. *Biol. Oceanogr.* 6, 443–461.

Ralph, P. J., and Gademann, R. (2005). Rapid light curves: a powerful tool to assess photosynthetic activity. *Aquat. Bot.* 82, 222–237. doi: 10.1016/j.aquabot.2005.02.006

Raven, J. A., Evans, M. C. W., and Korb, R. E. (1999). The role of trace metals in photosynthetic electron transport in O-2-evolving organisms. *Photosynth. Res.* 60, 111–149. doi: 10.1023/a:1006282714942

Raven, J. A., and Kubler, J. E. (2002). New light on the scaling of metabolic rate with the size of algae. *J. Phycol.* 38, 11–16. doi: 10.1046/j.1529-8817.2002.01125.x

Saito, M. A., and Goepfert, T. J. (2008). Zinc-cobalt colimitation of *Phaeocystis antarctica*. *Limnol. Oceanogr.* 53, 266–275. doi: 10.4319/lo.2008.53.1.0266

Saito, M. A., Goepfert, T. J., and Ritt, J. T. (2008). Some thoughts on the concept of colimitation: three definitions and the importance of bioavailability. *Limnol. Oceanogr.* 53, 276–290. doi: 10.4319/lo.2008.53.1.0276

Saito, M. A., Moffett, J. W., Chisholm, S. W., and Waterbury, J. B. (2002). Cobalt limitation and uptake in *Prochlorococcus*. *Limnol. Oceanogr.* 47, 1629–1636. doi: 10.4319/lo.2002.47.6.1629

Sañudo-Wilhelmy, S. A., Cutter, L. S., Durazo, R., Smail, E. A., Gómez-Consarnau, L., Webb, E. A., et al. (2012). Multiple B-vitamin depletion in large areas of the coastal ocean. *Proc. Natl. Acad. Sci. U.S.A.* 109, 14041–14045. doi: 10.1073/pnas.1208755109

Schuback, N., Schallenberg, C., Duckham, C., Maldonado, M. T., and Tortell, P. D. (2015). Interacting effects of light and iron availability on the coupling of photosynthetic electron transport and CO2-assimilation in marine phytoplankton. *Plos One* 10:e0133235. doi: 10.1371/journal.pone.0133235

Shaked, Y., and Lis, H. (2012). Disassembling iron availability to phytoplankton. *Front. Microbiol.* 3:123. doi: 10.3389/fmicb.2012.00123

Sinoir, M., Bowie, A. R., Mongin, M., Butler, E. C. V., and Hassler, C. S. (2017). Zinc requirement for two phytoplankton strains of the Tasman Sea. *Mar. Freshw. Res.* 68, 361–372. doi: 10.1071/mf15323

Sinoir, M., Butler, E. C. V., Bowie, A. R., Mongin, M., Nesterenko, P. N., and Hassler, C. S. (2012). Zinc marine biogeochemistry in seawater: a review. *Mar. Freshw. Res.* 63, 644–657. doi: 10.1071/mf11286

Strzepek, R. F., Hunter, K. A., Frew, R. D., Harrison, P. J., and Boyd, P. W. (2012). Iron-light interactions differ in Southern Ocean phytoplankton. *Limnol. Oceanogr.* 57, 1182–1200. doi: 10.4319/lo.2012.57.4.1182

Strzepek, R. F., Maldonado, M. T., Hunter, K. A., Frew, R. D., and Boyd, P. W. (2011). Adaptive strategies by Southern Ocean phytoplankton to lessen iron limitation: uptake of organically complexed iron and reduced cellular iron requirements. *Limnol. Oceanogr.* 56, 1983–2002. doi: 10.4319/lo.2011.56.6.1983

Suggett, D. J., Moore, C. M., Hickman, A. E., and Geider, R. J. (2009). Interpretation of fast repetition rate (FRR) fluorescence: signatures of phytoplankton community structure versus physiological state. *Mar. Ecol. Prog. Ser.* 376, 1–19. doi: 10.3354/meps07830

Sunda, W. G. (2012). Feedback interactions between trace metal nutrients and phytoplankton in the ocean. *Front. Microbiol.* 3:204. doi: 10.3389/fmicb.2012.00204

Sunda, W. G., and Huntsman, S. A. (1992). Feedback interactions between zinc and phytoplankton in seawater. *Limnol. Oceanogr.* 37, 25–40. doi: 10.1038/ismej.2010.211

Sunda, W. G., and Huntsman, S. A. (1995). Cobalt and zinc interreplacement in marine phytoplankton: biological and geochemical implications. *Limnol. Oceanogr.* 40, 1404–1417. doi: 10.4319/lo.1995.40.8.1404

Sunda, W. G., and Huntsman, S. A. (1998). Processes regulating cellular metal accumulation and physiological effects: Phytoplankton as model systems. *Sci. Total Environ.* 219, 165–181. doi: 10.1016/s0048-9697(98)00226-5

Sunda, W. G., and Huntsman, S. A. (2004). Relationships among photoperiod, carbon fixation, growth, chlorophyll a, and cellular iron and zinc in a coastal diatom. *Limnol. Oceanogr.* 49, 1742–1753. doi: 10.4319/lo.2004.49.5.1742

Tang, Y. Z., Koch, F., and Gobler, C. J. (2010). Most harmful algal bloom species are vitamin B-1 and B-12 auxotrophs. *Proc. Natl. Acad. Sci. U.S.A.* 107, 20756–20761. doi: 10.1073/pnas.1009560107

Timmermans, K. R., Snoek, J., Gerringa, L. J. A., Zondervan, I., and de Baar, H. J. W. (2001). Not all eukaryotic algae can replace zinc with cobalt: *Chaetoceros calcitrans* (Bacillariophyceae) versus *Emiliania huxleyi* (Prymnesiophyceae). *Limnol. Oceanogr.* 46, 699–703. doi: 10.4319/lo.2001.46.3.0699

Trimborn, S., Thoms, S., Bischof, K., and Beszteri, S. (2019a). Susceptibility of two Southern Ocean phytoplankton key species to iron limitation and high light. *Front. Mar. Sci.* 6:167. doi: 10.3389/fmars.2019.00167

Trimborn, S., Thoms, S., Karitter, P., and Bischof, K. (2019b). Ocean acidification and high irradiance stimulate growth of the Antarctic cryptophyte *Geminigera cryophila*. *Biogeosci. Rev.* 16, 2997–3008.

Trimborn, S., Thoms, S., Brenneis, T., Heiden, J. P., Beszteri, S., and Bischof, K. (2017). Two Southern Ocean diatoms are more sensitive to ocean acidification and changes in irradiance than the prymnesiophyte Phaeocystis antarctica. *Physiol. Plant.* 160, 155–170. doi: 10.1111/ppl.12539

Turpin, D. H. (1991). Effects of inorganic N availability on algal photosynthesis and carbon metabolism. *J. Phycol.* 27, 14–20. doi: 10.1111/j.0022-3646.1991.00014.x

Turpin, D. H., Elrifi, I. R., Birch, D. G., Weger, H. G., and Holmes, J. J. (1988). Interactions between photosynthesis, respiration and nitrogen assimilation in microalgae. *Can. J. Bot.* 66, 2083–2097. doi: 10.1139/b88-286

Twining, B. S., and Baines, S. B. (2013). "The Trace Metal Composition of Marine Phytoplankton," in *Annual Review of Marine Science*, Vol. 5, eds C. A. Carlson and S. J. Giovannoni (Palo Alto, CA: Annual Reviews), 191–215. doi: 10.1146/annurev-marine-121211-172322

van Leeuwe, M. A., and Stefels, J. (1998). Effects of iron and light stress on the biochemical composition of Antarctic *Phaeocystis* sp. *(Prymnesiophyceae)*. II. Pigment composition. *J. Phycol.* 34, 496–503. doi: 10.1046/j.1529-8817.1998.340496.x

van Leeuwe, M. A., and Stefels, J. (2007). Photosynthetic responses in *Phaeocystis antarctica* towards varying light and iron conditions. *Biogeochemistry* 83, 61–70. doi: 10.1007/s10533-007-9083-5

Varela, D. E., Willers, V., and Crawford, D. W. (2011). Effect of zinc availability on growth, morphology, and nutrient incorporation in a coastal and an oceanic diatom. *J. Phycol.* 47, 302–312. doi: 10.1111/j.1529-8817.2010.00948.x

Vergara, J. J., Berges, J. A., and Falkowski, P. G. (1998). Diel periodicity of nitrate reductase activity and protein levels in the marine diatom *Thalassiosira weissflogii* (Bacillariophyceae). *J. Phycol.* 34, 952–961. doi: 10.1046/j.1529-8817.1998.340952.x

Wake, B. D., Hassler, C. S., Bowie, A. R., Haddad, P. R., and Butler, E. C. V. (2012). Phytoplanktotn selenium requirements: the case for species isolated from temperate and polar regions of the southern hemisphere. *J. Phycol.* 48, 585–594. doi: 10.1111/j.1529-8817.2012.01153.x

Wright, S. W., Jeffrey, S. W., Mantoura, R. F. C., Llewellyn, C. A., Bjornland, T., Repeta, D., et al. (1991). Improved HPLC method for the analysis of chlorophylls and carotenoids from marine-phytoplankton. *Mar. Ecol. Prog. Ser.* 77, 183–196. doi: 10.3354/meps077183

Wuttig, K., Townsend, A. T., van der Merwe, P., Gault-Ringold, M., Holmes, T., Schallenberg, C., et al. (2019). Critical evaluation of a seaFAST system for the analysis of trace metals in marine samples. *Talanta* 197, 653–668. doi: 10.1016/j.talanta.2019.01.047

Xu, Y., Tang, D., Shaked, Y., and Morel, F. M. M. (2007). Zinc, cadmium, and cobalt interreplacement and relative use efficiencies in the coccolithophore *Emiliania huxleyi*. *Limnol. Oceanogr.* 52, 2294–2305. doi: 10.4319/lo.2007.52.5.2294

Conflict of Interest Statement: The authors declare that the research was conducted in the absence of any commercial or financial relationships that could be construed as a potential conflict of interest.